Technical Report Documentation Pag

1. Report No. FHWA-RD-78-45	2. Government Accession No.	3. Recipient's Catalog No. PB291296
4. Title and Subtitle "Appraisal Of Techniques To Reduce Embedment Friction While Post-Stressing Concrete" Final Report		5. Report Date 10 March 1978 6. Performing Organization Code 8. Performing Organization Report No.
7. Author(s) Ronald W. Chandler, Robert K. Brownlow, David Johnson		
9. Performing Organization Name and Address Tetradyne Corporation 1681 South Broadway Carrollton, Texas 75006		10. Work Unit No. (TRAIS) FCP 35E3032 11. Contract or Grant No. DOT-FH-11-8894
12. Sponsoring Agency Name and Address Department of Transportation Federal Highway Administration Office of Contracts and Procurement Washington, D.C. 20590		13. Type of Report and Period Covered Final Report 14. Sponsoring Agency Code S0794

15. Supplementary Notes

FWHA contract manager, Dr. T.F. McMahon, HRS-14

16. Abstract

In this report, two concepts for reducing friction losses along post-tensioned tendons in pavement slabs are studied. One concept involved the use of vibration techniques to increase stressing efficiency, and the other concept included the reduction of friction coefficient through the use of a material which would also act as a grout after stressing the tendon.

For the vibration techniques, three vibration systems were constructed and tested. One was based on the use of hydraulic pressure pulsations to cause a sharp jerking action on a tendon. The desired effect was not accomplished with the system constructed.

The other two systems used impact generated vibrations, which affected normal forces along the tendons. The impact vibrations did produce changes in the friction losses but not that which would be desirable for post-tensioned tendons in long pavement slabs.

Grout materials tested were two, 2-part and two heat cure epoxy resins. Tendon heating through the use of an AC arc welder was also investigated in order to determine the feasibility of this method for setting the heat cure epoxies. The results of these tests were inconclusive but do show promise for future investigations.

17. Key Words Friction reduction, coefficient of friction, hydraulic vibration, impact, normal forces, applied tension, anchor tension.	18. Distribution Statement No restrictions. This document is available to the public through the National Technical Information Service, Springfield, Virginia 22161

19. Security Classif. (of this report) Unclassified	20. Security Classif. (of this page) Unclassified	21. No. of Pages 92	22. Price PCA05

Form DOT F 1700.7 (8-72) Reproduction of completed page authorized

LIST OF ILLUSTRATIONS

List of Illustrations (Continued)

List of Illustrations (Concluded)

LIST OF TABLES

List of Tables (Concluded)

I. CONCLUSIONS

Though the investigations of this report did not produce the hoped for results, much insight has been gained for future research into the areas of epoxy grouts, heat setting techniques, and vibration methods of reducing friction forces.

The attempt to reduce friction losses using a hydraulic vibration system was unsuccessful because the hydraulic system constructed for this study was not able to produce the sharp hydraulic pulses necessary to apply the desired loading action on the tendon. This is still a viable technique, however, with the proper hydraulic apparatus. This apparatus would not necessarily involve a large or complex hydraulic system and is worthy of continued investigation.

The impact technique did produce increases in tension at the anchor end where the impact was applied but did not have the overall desired effects on the tendon stress distribution. A large enough impact force allowed the tendon to slip in the direction of the applied tension with an overall lowering of the tension along the tendon. The resulting elastic oscillation stressed and relaxed the tendon over several cycles leaving a harmonically varying stress distribution along the tendon of decreasing amplitude toward the anchor end.

Heat setting epoxies still may offer some advantage in reduction of friction coefficient, but there are other critical areas which need to be

investigated; creep, volume change, final pumpable consistency with filler added, and handling problems.

Heat setting methods show some promise although the method is evidently vulnerable to unfavorable environmental conditions. The insulating effect of the epoxy grout would need to be established.

II. RECOMMENDATIONS

Thermoplastic resins were dropped from investigation because the data researched showed no thermoplastic resin with all of its properties compatible for the application under investigation. However, since thermoplastic materials are so numerous and involve a great amount of technology, further investigation is recommended.

For possible future tests using a hydraulic apparatus to increase stressing efficiency, the apparatus of Figure 1 is recommended as a possible mechanism to generate the required hydraulic pulses. It simply involves an external impact force on a small diameter hydraulic piston connected to the stressing ram as shown. If necessary, controllability of the impact force could be developed, but for initial feasibility studies, a mass dropped from various heights could be a sufficient method.

Another method of reducing friction which was discussed, but which was outside the scope of this project, was the reduction of wobble curvature through the use of channel to support the plastic encased tendon. The plastic encased tendon was tested in rigid conduit but the friction loss was found to be worse because the plastic case deformed and sheared open. If, however, a fairly rigid plastic channel were used to support the tendon, wobble would be greatly reduced and the plastic case would not deform so easily within the tight cement enclosure. The final stressing efficiency could be raised significantly if the lower friction coefficients offered by

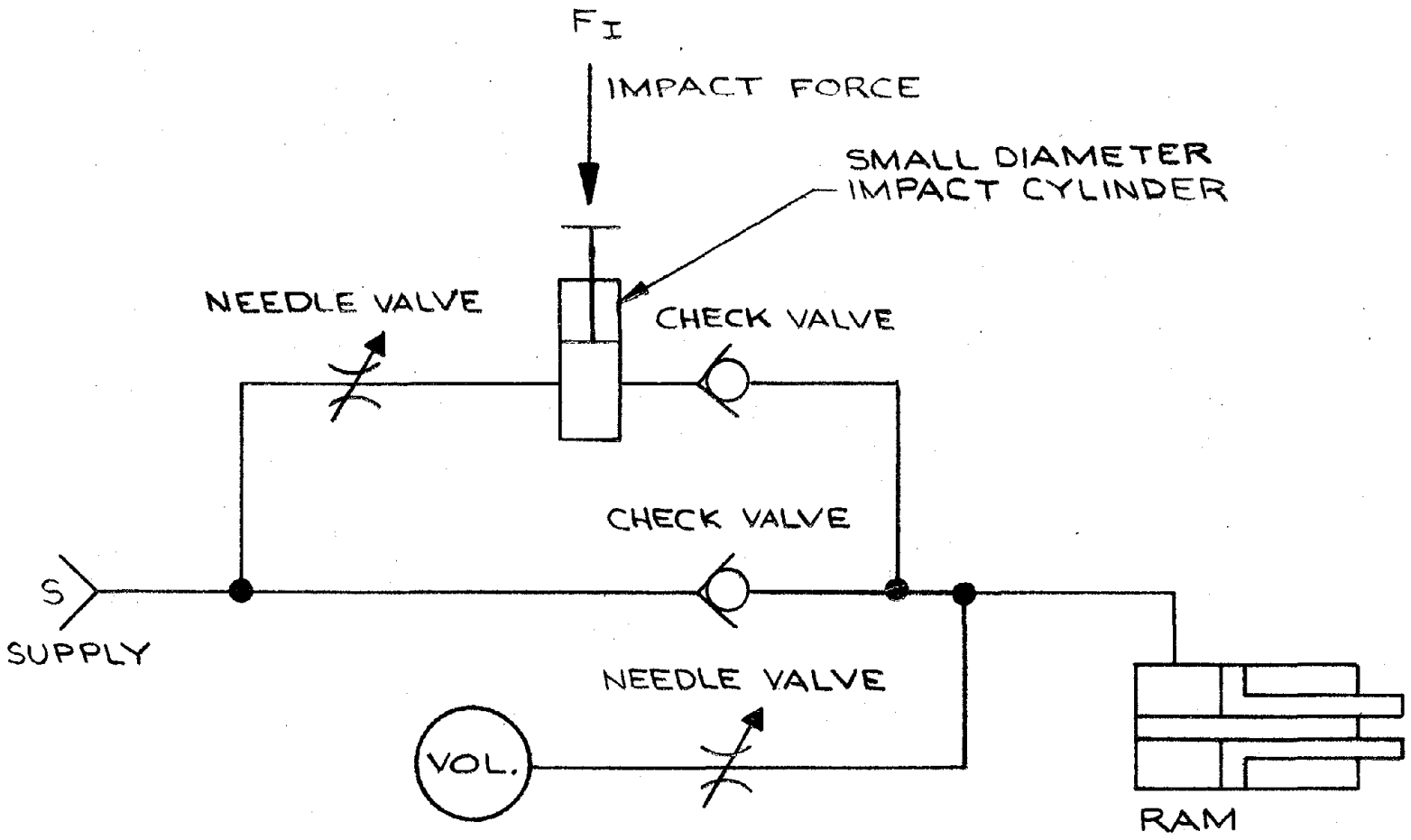

(a) Schematic of System

FIGURE 1 . SUGGESTED HYDRAULIC IMPACT SYSTEM FOR FUTURE FRICTION LOSS REDUCTION STUDIES.

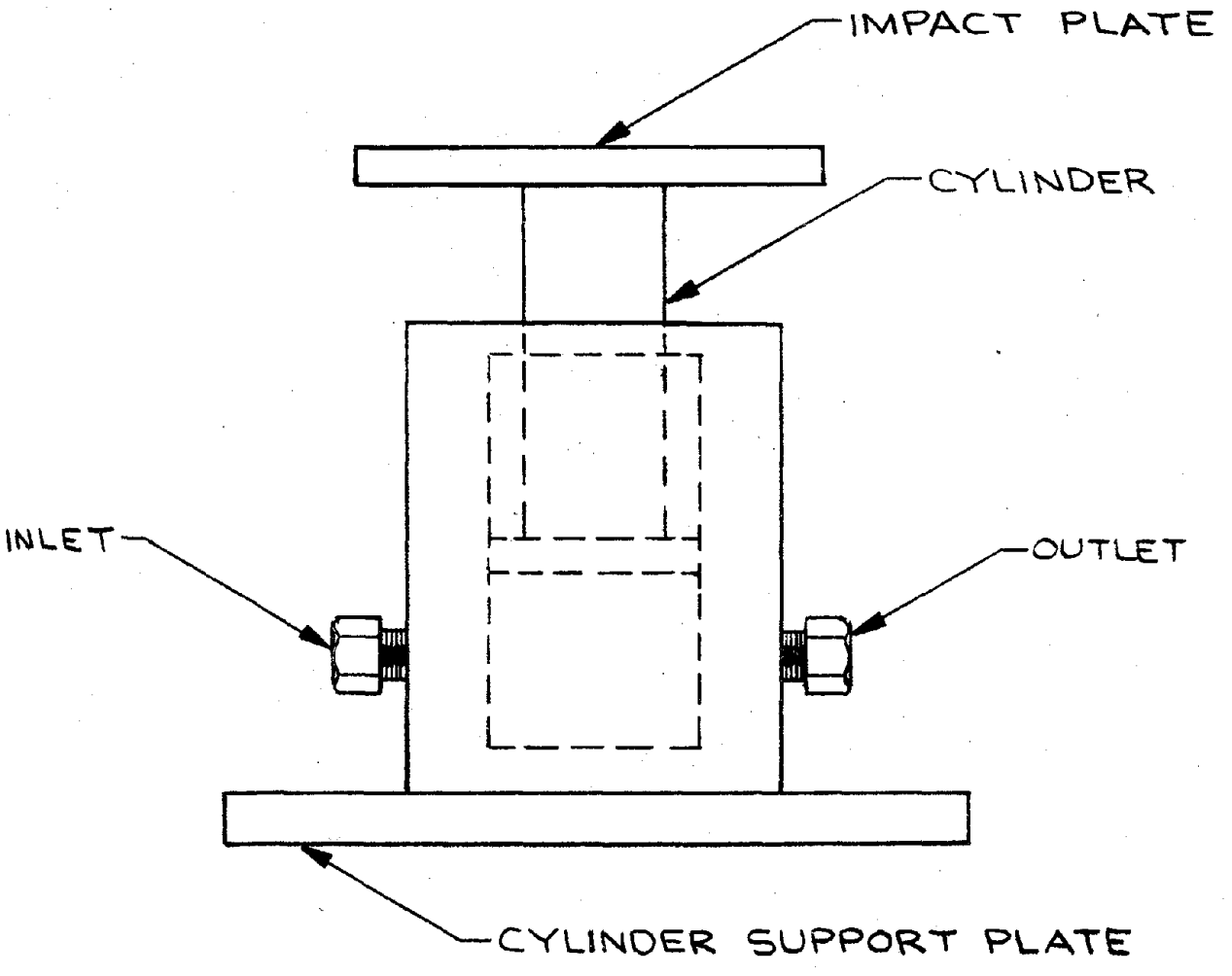

(b) Schematic of Small Diameter Impact Cylinder

Figure 1. SUGGESTED HYDRAULIC IMPACT SYSTEM FOR FUTURE FRICTION LOSS REDUCTION STUDIES. (Continued)

the plastic encased tendon were coupled with large reductions in wobble curvature induced by normal forces, as could be obtained if the tendons were supported. This method would not only be practical, but easily applicable and economical as compared to the steel conduit. Figure 2 shows the tendon-channel concept.

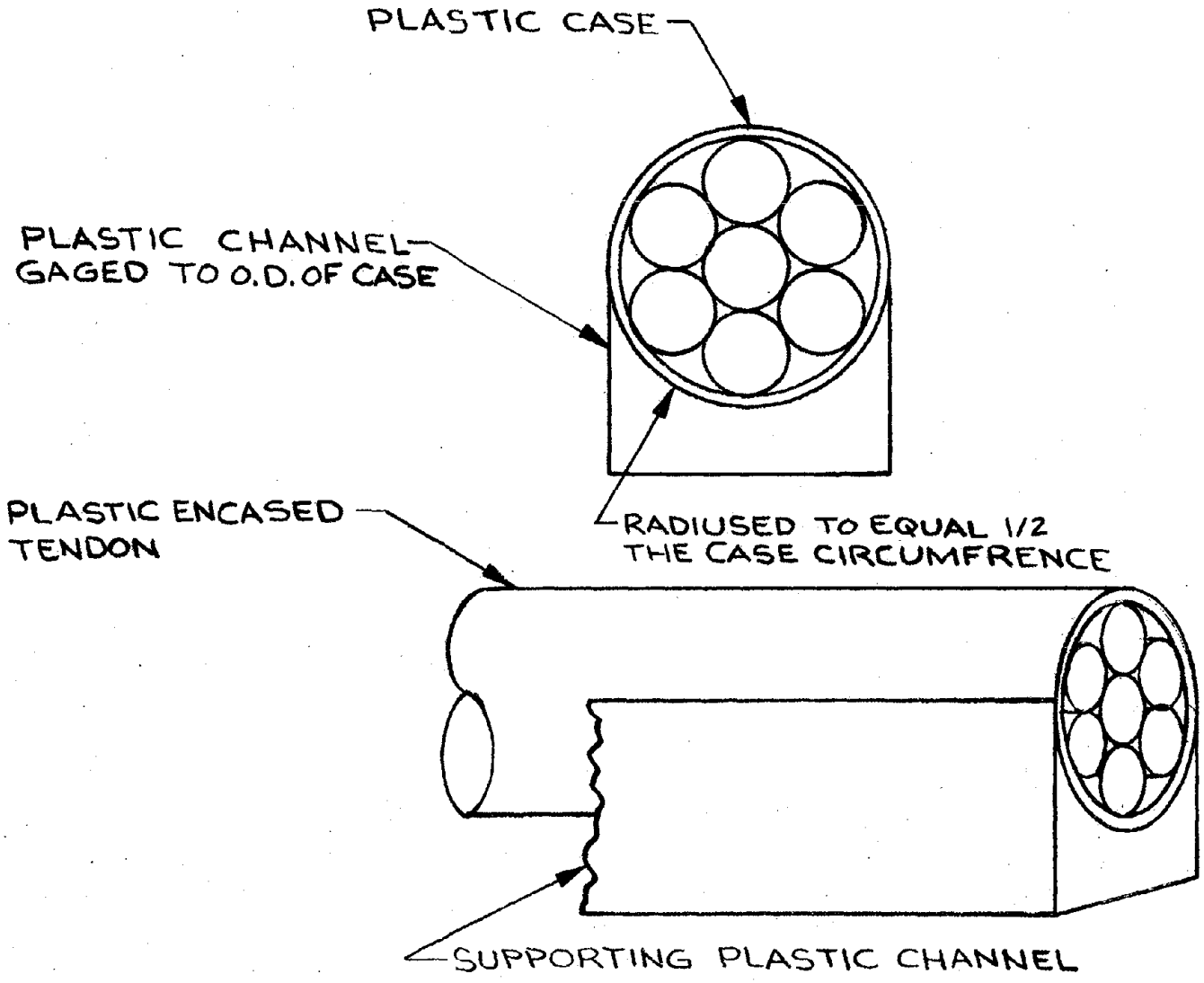

FIGURE 2. PLASTIC CHANNEL CONCEPT.

III. INTRODUCTION

A. Problems Imposed by Friction Losses

An important problem in the design of prestressed pavements concerns the curvature induced friction losses along post-tensioned tendons together with the resulting limitations imposed on structual integrity and length of maintenance-free operation in long slab designs. Friction losses from 15 pounds/foot (219 Newton/meter) for bare tendon in rigid steel tubing to 40 pounds/foot (584 Newton/meter) for plastic encased tendons have been reported.[1] These losses become critical in slabs of 400-foot (122 meter) lengths or more.

B. Approaches to Problem

Two concepts for reducing friction losses along tendons in steel conduits were investigated in this study. One approach involved the reduction of friction coefficient in steel conduit through the use of lubricating resins which would also serve as grouts after the final stressing operation was completed. The other approach was aimed at reduction of normal forces by inducing longitudinal vibrations into stressed tendons.

[1] "Prestressed Concrete Pavement at Dulles International Airport: Research Report to 100 Days" - B.F. Friberg and T.J. Pasko, August, 1973, Interim Report, Report No. FHWA-RD-72-29, Federal Highway Administration Offices of Research and Development, Washington, D.C.

IV. TESTING APPARATUSES

A. Concrete Test Blocks

There were two phases of friction reduction studies utilizing concrete test blocks. The first phase involved the testing of a hydraulic vibration apparatus with standard tendon-conduit configurations. In the second phase, various resin grouts and impact vibration methods were tested for their friction reduction potential on tendons in rigid and flexible steel conduits.

1. First Friction Studies. For the first friction studies involving the hydraulic vibrator, the test block was designed to allow testing of the standard configurations of a bare tendon in rigid conduit as well as a plastic encased pregreased tendon. The conduit and plastic encased tendon were arranged to have a 90° arc with a three-foot (0.91 meter) radius so that there would be a substantial friction loss along the tendons. Allowance was also made for a straight-through conduit and plastic encased tendon for calibration and comparison purposes. Figure 3 is a diagram of the test block and is based on a design used by Guyon.[2] Figure 4 (a) shows the conduit, tendons and reinforcement in the form. Figure 4 (b) shows the finished block with testing apparatus for the hydraulic vibrator.

---

[2] "Prestressed Concrete - V. Guyon, 1953, John Wiley and Sons, Inc.

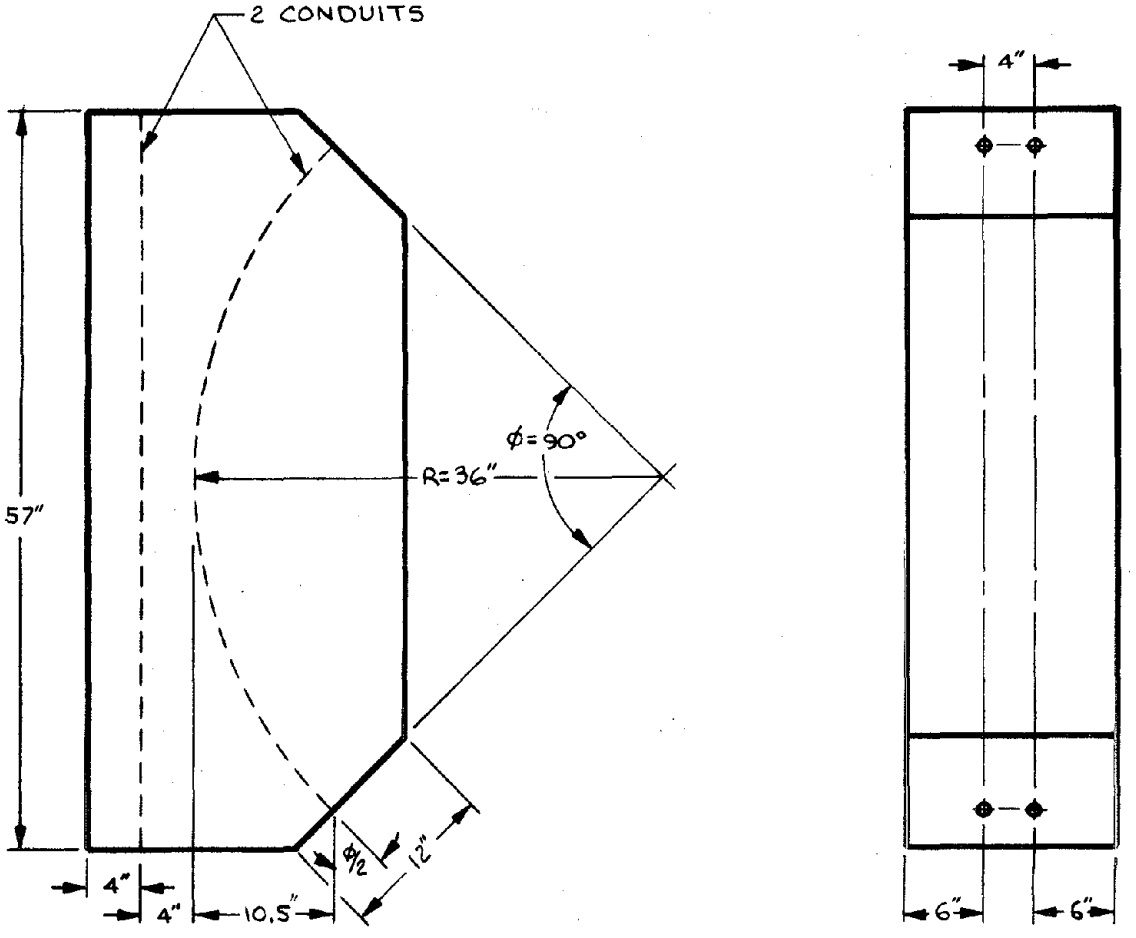

(1" = 25.4 mm)

FIGURE 3. CONCRETE TEST BLOCK FOR FRICTION STUDIES WITH HYDRAULIC VIBRATOR.

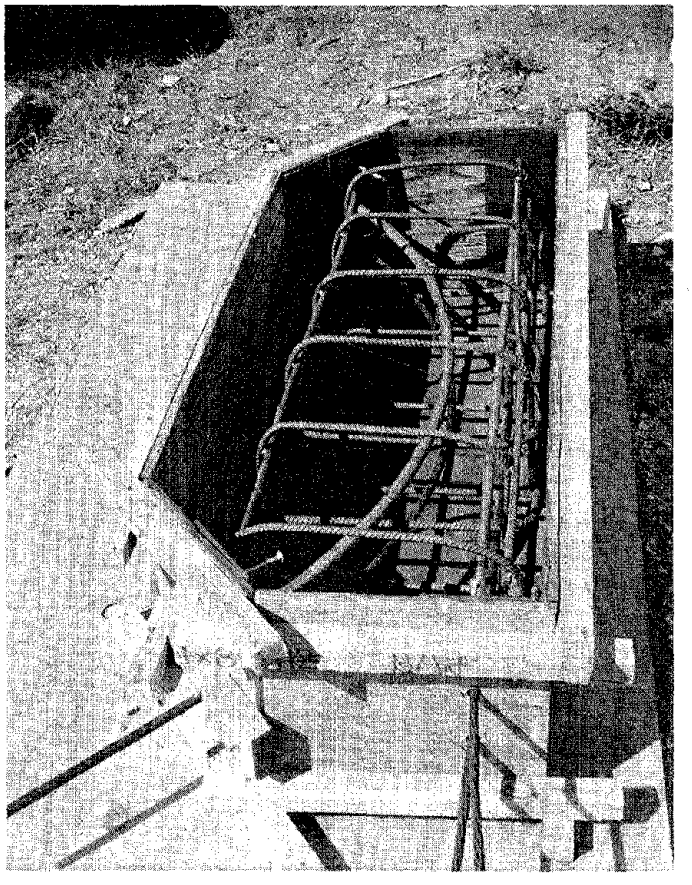

(a). Form Ready for Concrete

FIGURE 4. CONSTRUCTION OF TEST BLOCK FOR HYDRAULIC VIBRATOR TESTS.

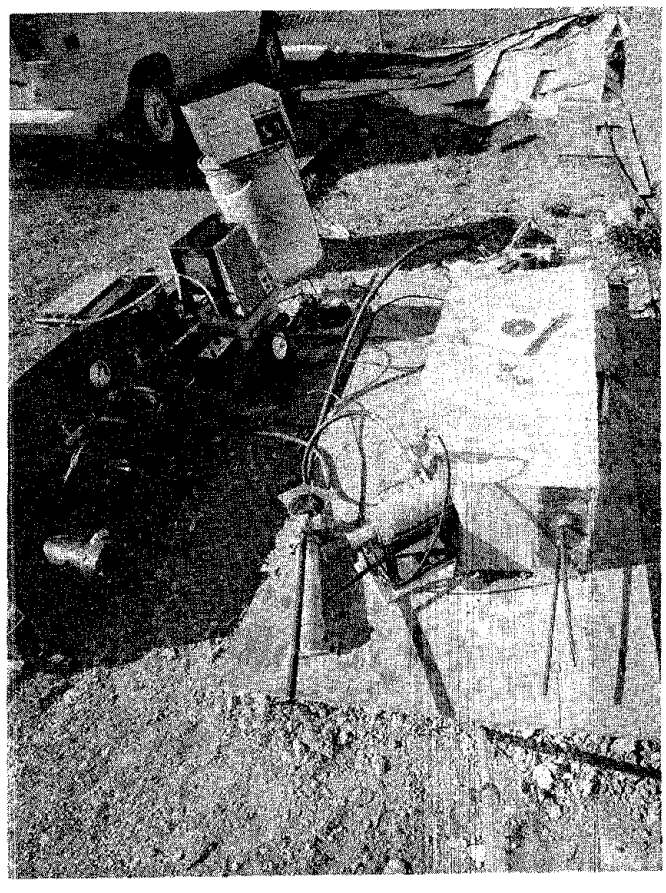

(b). Tests Under Way

FIGURE 4. CONSTRUCTION OF TEST BLOCK FOR HYDRAULIC VIBRATOR TESTS. (Continued)

2. Resin Grout and Impact Studies. Test blocks for the resin grout and impact studies were similar to the first block but designed to allow six conduits in each block in sets of three each of either rigid or flexible conduit. Figure 5 (a) shows a form on its sand base with support bars and anchor plates ready for installation. Figure 5 (b) shows a completed form with rigid conduits installed. The flexible conduits were supported and fixed in position by wiring them into halved sections of rigid conduits as shown in Figure 5 (c). The rigid conduit used was .75-inch (1.9 centimeter) inside diameter electro-metallic tubing (E.M.T.) electrical conduit with a .047-inch (0.12 centimeter) wall thickness. The flexible conduit used was .625-inch (1.59 centimeter) inside diameter spiral wound electrical conduit also with a .047-inch (0.12 centimeter) wall thickness. Tendons used in all the tests were nine feet sections of either bare or plastic encased pregreased tendons with a .153 square inch (.987 square centimeter) cross section and 270,000 pounds per square inch (1.862×10^9 paschal) ultimate strength.

B. Stressing System

Stressing was accomplished through the use of an Enerpac 10,000 psi (6.895×10^7 paschal) pump and two Enerpac 30-ton (4.137×10^8 paschal) rams. Two Templeton-Kenley 15,000 psi (1.034×10^8paschal) pressure gauges with a $\pm$ 100 psi (6.895×10^5 paschal) readability were used. One was used to check the pressure at the applied load end of the tendon and the other to check the pressure in the ram at the anchor end of the tendon. A specially

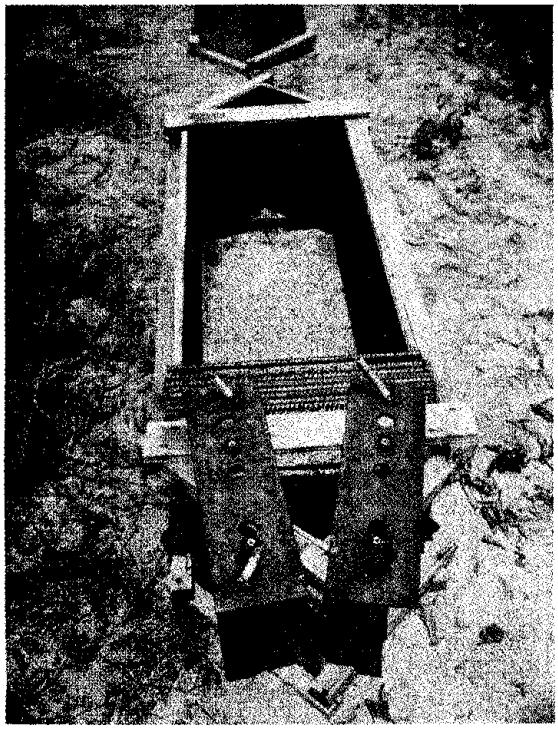

(a) Support Bars and Anchor Plates Ready for Installation

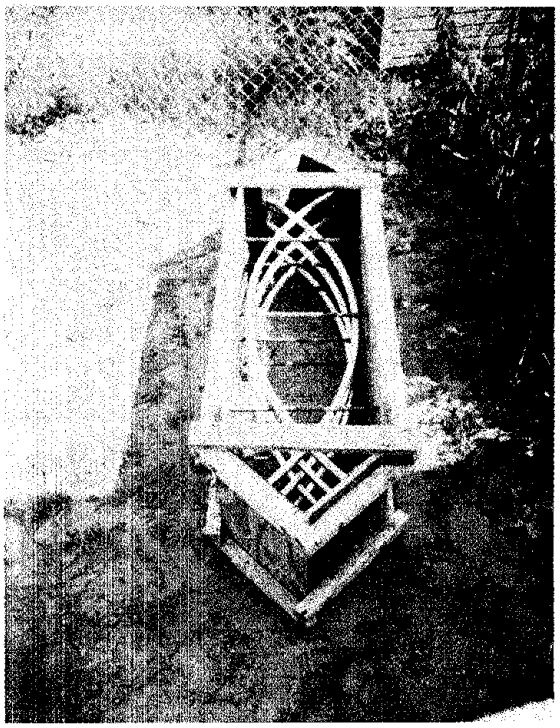

(b) Completed Form With Rigid Conduit

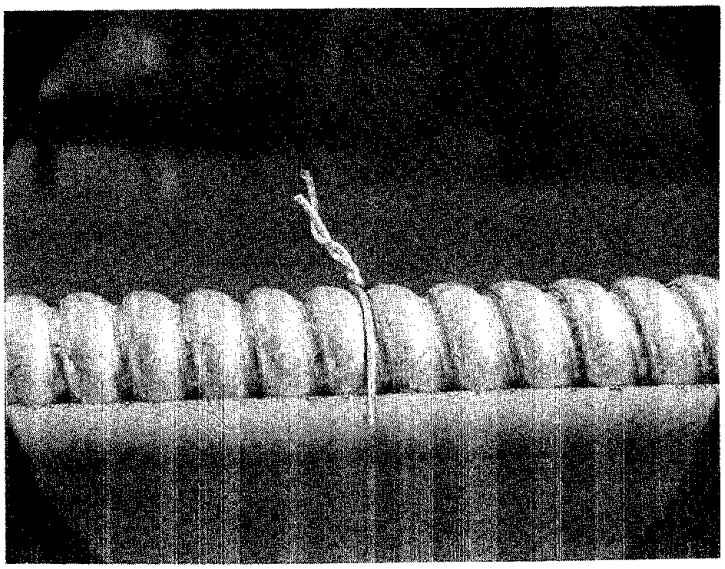

(c) Support for Flexible Conduit

FIGURE 5. CONSTRUCTION OF TEST BLOCKS FOR RESIN GROUT AND IMPACT STUDIES.

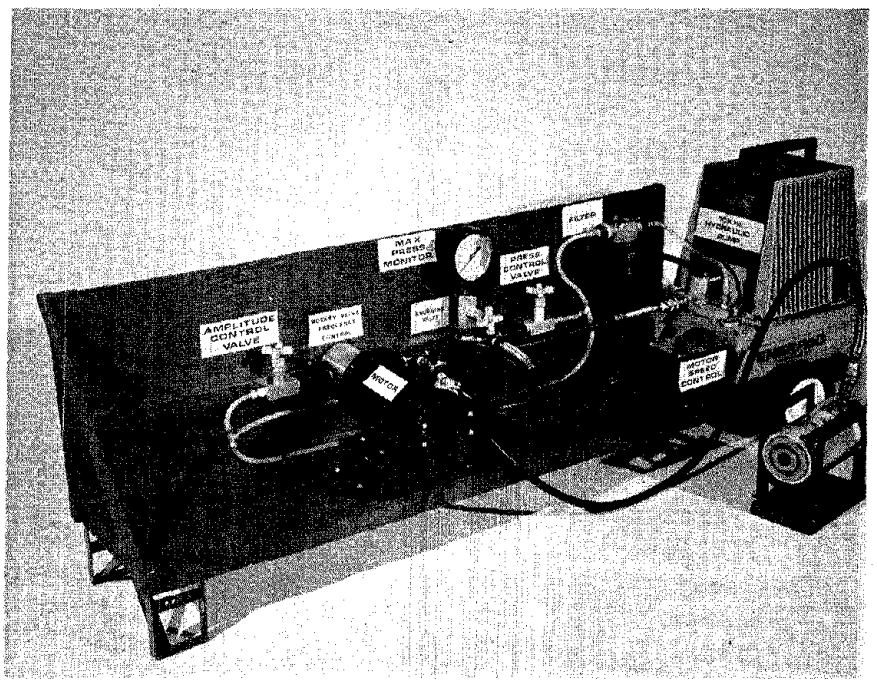

FIGURE 6. HYDRAULIC VIBRATOR SYSTEM WITH ROTARY VALVE.

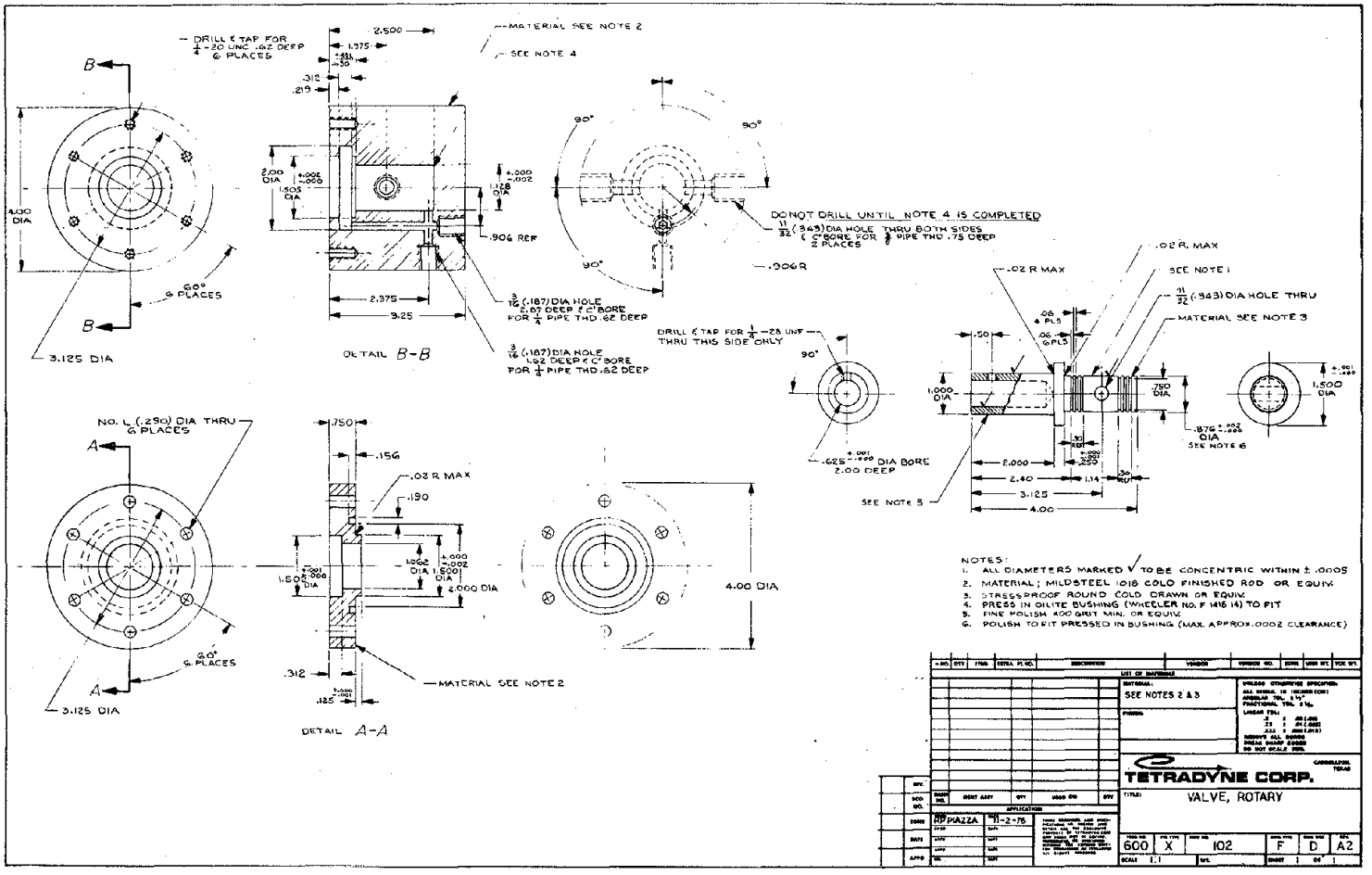

FIGURE 7. ASSEMBLY BLUEPRINT DRAWING OF ROTARY VALVE.

designed rotary valve was used in the first friction studies and is shown in Figure 6 with the rest of the hydraulic system. Figure 7 shows the valve and rotor design.

The original hydraulic system was modified to perform the impact studies of the second series of friction tests. A 5,000 psi (3.447×10^7 paschal) reducing valve was added to the system, along with a Marsh 10,000 psi (6.895×10^7 paschal) pressure gauge with a ± 50 psi (3.447×10^5 paschal) readability, to monitor the applied load hydraulic pressure. The reducing valve served to filter pump pressure fluctuations at higher pressures. It also allowed much more efficient control of the system pressure levels. Figure 8 shows the modified hydraulic system for the impact studies.

C. Vibration Systems

1. Hydraulic Vibrator Rotary Valve System. Initially, friction reduction was attempted through the application of stress waves, of relaxation-tension-relaxation form in the direction of applied load at the loading or "live" end of the test block. The stress waves were generated with the use of a rotary valve driven by a variable speed DC motor. The ram pressure dropped whenever the turning valve rotor orifice became aligned with the by-pass ports in the valve body (refer to Figures 6 and 7). After the orifice passed the ports, the system was again closed and the ram pressure would increase. The result was a relaxation-tension-relaxation cycle where the frequency could be varied by a variation of the motor RPM.

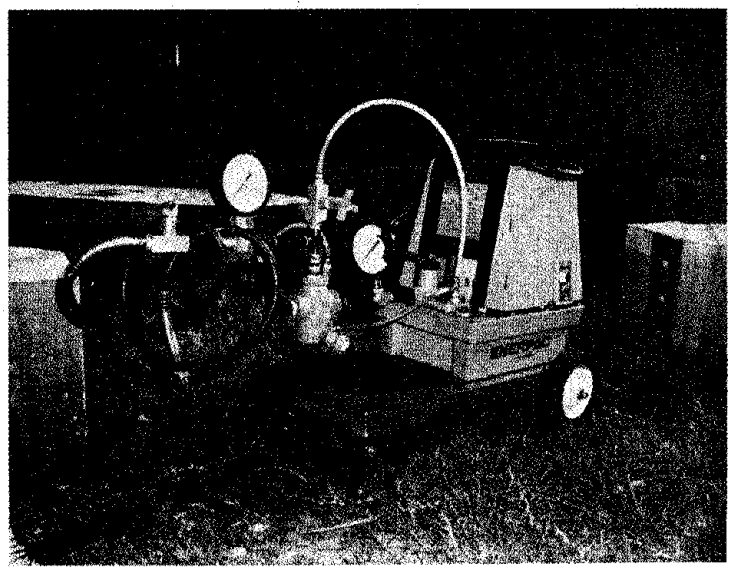

FIGURE 8. HYDRAULIC SYSTEM FOR IMPACT STUDIES.

The envisioned result was to be able to apply a jerking action to the tendon in an effort to overcome the frictional resistance.

2. Impact Methods. The second method of attempting friction reduction also used the relaxation-tension cycle but was applied at the "anchor" end of the test block. In this case, in order to provide the sharp jerking motion desired, a hammer blow type impact was used. Two different systems were employed to provide the impact.

a. Pneumatic. The first system incorporated an industrial pneumatic impact vibrator. Impact was provided by a sliding piston accelerated by a charge of air from a time controlled pneumatic valve. A constant low level air pressure returned the piston to its starting point.

b. Impact Pendulum. The second system was a simple pendulum motion impact hammer. The pendulum length could be varied, allowing variation of the impact velocity. The hammer mass could also be varied, using lead shot. The lead shot had the advantage of suppressing the rebound velocity and increasing the impact duration time.

D. Data Collection System

1. Sensing Devices. Sensing devices used in the tests included BLH .5,000 psi (3.447×10^7 paschal) pressure transducers and Houston Scientific 50,000-pound (2.224×10^5 Newton) load cells. The pressure transducers were used with the rotary valve hydraulic vibration system while the load cells were used for the impact tests. A hydraulic pressure of 5,000 psi (3.447×10^7 paschal) was equivalent to a 30,000-pound (1.334×10^5

Newton) tensile load on the tendons.

2. Recording Equipment. The recording equipment used was a Honeywell 1858 Visicorder and modular inserts of the type necessary to interface the sensing devices. The Visicorder allowed graphical recordings of .0125 second/inch (4.921×10^{-3} second/centimeter) for the stress wave analysis of the different vibration systems.

V. TESTING AND EVALUATION OF FRICTION REDUCTION CONCEPTS

A. Hydraulic Rotary Valve System

1. Controllability. The rotary valve system had the advantages of good controllability within the set limits. Hydraulic pulse amplitudes could be controlled by orifice size and motor speed as well as the set pressure level. The peak-to-peak stress amplitude could be as much as 70 percent of the set level at lower frequencies. Another advantage was good repeatability of the pulse magnitudes.

2. Limiting Factors. There were several limiting factors on the performance of the system. One factor was that the flow rate decreased with increasing pressure, resulting in a slow pressure rise with a sharp drop. The desired affect was a sharp rise and a sharp drop. The slow rise characteristic also limited the maximum pressures obtainable at higher pulse rates.

Another factor was that the peak pulse amplitude could be no more than the set pressure level. It would be more desirable for the pulses to oscillate "around" the set level rather than below the set level.

Other limiting factors on the system performance involved the increase in normal forces with increase in tension. This meant that the slow rise in tension could achieve really no more than the theoretical efficiency for a given curvature and friction coefficient. A sharp pulse, however, might have the positive aspect of increasing the stressing efficiency even if the pulses oscillated below the set level.

3. Results. The results of the tests with the hydraulic vibration system reflect all the problem areas discussed above. Within the stated problems and geometric configuration of the tests, there was no observed increase in anchor tension. Figure 9 shows the pulse amplitudes versus frequency for five maximum tension levels. At the 30 kip (1.334×10^5 Newton) level, the hydraulic pressure would drop continuously below a frequency of about 2.5 cycles.

B. RESIN GROUTS

1. Grout Selection. Lubricating grouts for four structural combinations were considered. They were:

a. Tendon coated with remeltable thermoplastic resin.

b. Tendon sheathed in flexible conduit and precharged with viscous thermoset epoxy resin.

c. Rigid conduit with thermoset epoxy resin pumped in after stressing tendon.

d. Rigid conduit with 2-part epoxy resin pumped in after stressing tendon.

For the heat cure epoxies and the remeltable thermoplastic resins, a heat source would have been provided by connecting an AC arc welder to the ends of the tendon. Tests conducted with an AC arc welder connected to a 20-foot (6.1 meter) tendon showed that a fairly uniform temperature of

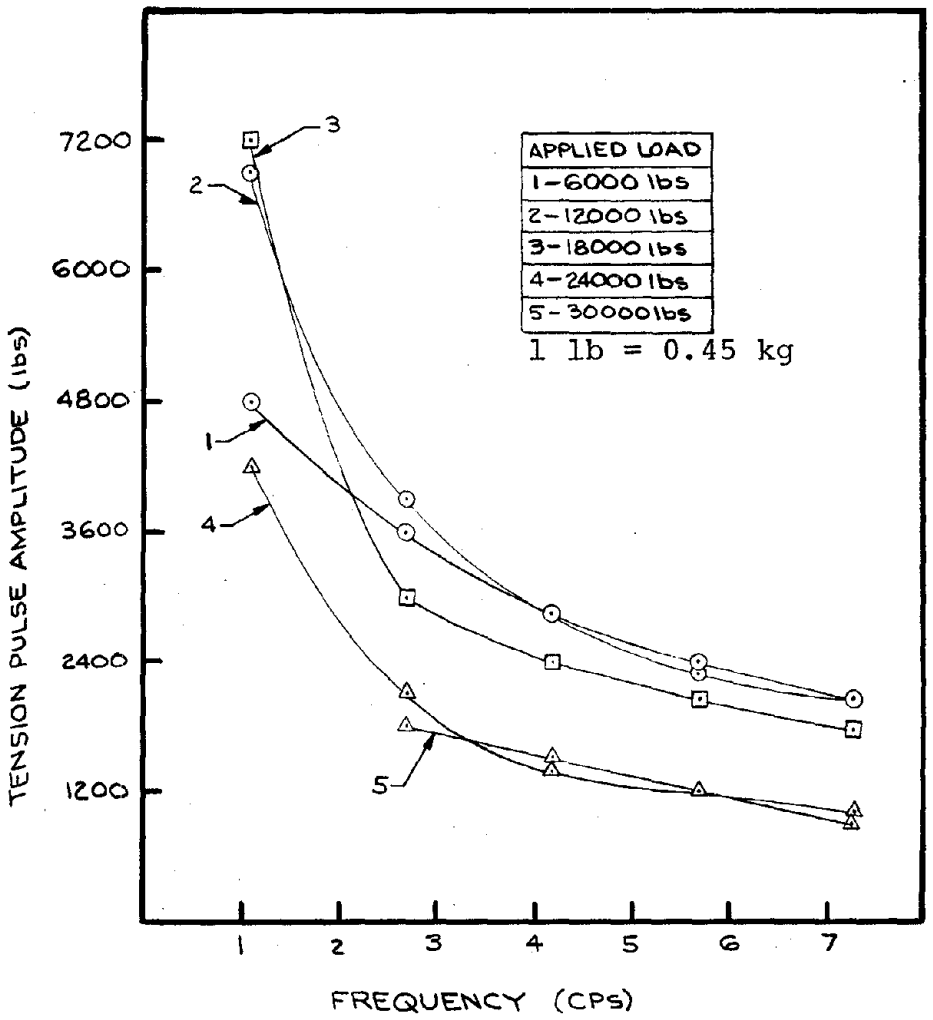

FIGURE 9. VIBRATIONAL PERFORMANCE OF HYDRAULIC VIBRATION SYSTEM.

300° - 330° F (149° - 166° C) could be maintained. In this temperature range, the heat cure epoxies selected for testing were specified to cure in one hour.

1) Thermoplastic Resins. Investigation into types of thermoplastic resins available for use in combination (a) listed above, revealed that few resins, if any, are available at the present time which approach the requirements for this application. The requirements imposed were:

a) Good flexibility at room temperature for coiling.

b) Low viscosity at melt temperature for tensioning purposes.

c) Low melt temperatures so as not to change strength properties of the tendon.

d) Low creep properties for grout integrity.

Temperature data [3] for post tensioning tendons showed that the maximum allowable temperatures for the steel tendons fall within the 325° - 400° F [4] (163° - 204° C) range. Melt temperatures for flexible thermoplastic resins also fall in this range, but their viscosties are high since large pressures are required for molding at the prescribed temperatures. The creep characteristics [4] of flexible thermoplastics are poor with respect to the imposed requirements. A higher strength glass-filled or fiber reinforced resin with better creep characteristics is usually more rigid. Reference 4 lists creep characteristics

---

[3] Post Tensioning Manual - Post Tensioning Institute, 1972, Prestressed Concrete Institute.

[4] Modern Plastics Encyclopedia, 77-78, McGraw Hill, Inc.

and other properties for diverse types of thermoplastic resins. Mostly on the basis of those data, it was decided to drop combination (a) from testing as far as the scope of this project was concerned.

2) Thermosetting Resins. For the remaining structural combinations, the imposed requirements were:

a) Two-part epoxy-resin.

- Pot life - a minimum of 20 minutes with one hour preferred.
- Cure time - 24 hours to reach minimum required bond strength.
- Bond strength - 200 psi minimum (1.379×10^6 paschal).
- Consistency - that of post-tensioning cement grout (minimum).

b) One part heat-cure epoxy resin.

- Shelf life - 30 days at $70^\circ - 80^\circ$ F ($21^\circ - 27^\circ$ C) (minimum).
- Cure time - 1 hour at 350° F (177°C) (maximum).
- Bond strength - 200 psi (1.379×10^6 paschal) (minimum).
- Consistency - that of post-tensioning grout (minimum).

From the materials survey and recommendations by the Engineering Department of a local chemical company, two heat cure epoxy resins and two 2-part epoxy resins were chosen for testing.

2) Filler Selection.

a) Economics, Availability, Geometry. Since the cost of the epoxies was expected to be high, two fillers were also selected for the tests. Silica flour was chosen since it is a standard filler and fly ash was chosen because of its availability, low cost and spherical shape. It was hoped that the spherical shape would aid friction reduction. Figure 10 shows drawings of the geometric shape of the fillers as seen under a microscope.

b) Laboratory Tests. One of the fillers was to be eliminated on the basis of laboratory tests for friction properties and compressive strength. The other filler and epoxy combinations were then to be evaluated for material properties for future specifications. Figure 11 shows the flow chart of tests which were to be performed.

As indicated on the flow chart, the first tests to be performed were consistency tests aimed at determining the filler-epoxy mix ratios which would compare with that of normal cement grout. The local testing laboratory contracted for the tests, compared the epoxy consistencies against grout mixtures containing too much water. This caused the epoxy consistency to compare too high for establishment of filler-epoxy mix ratios in the specified range. As a result, they elected to perform the remaining tests using a one-to-one mix ratio. Test results as reported by the testing laboratory are listed in Table 1. Glass beads, or "oil-well prop" as

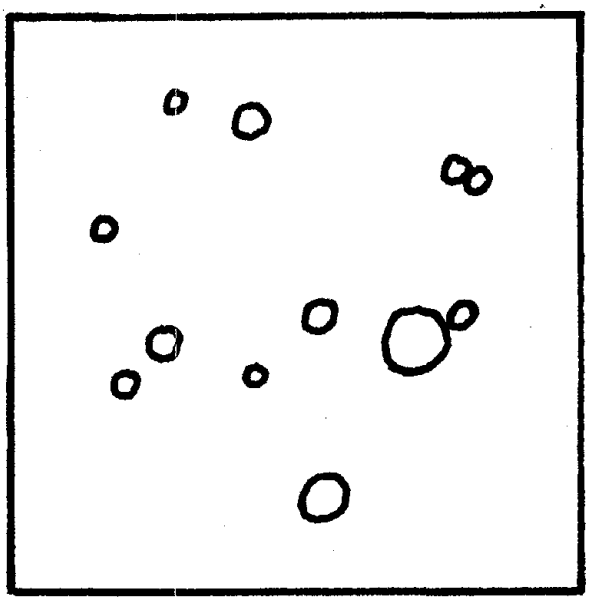

1200X
Fly Ash

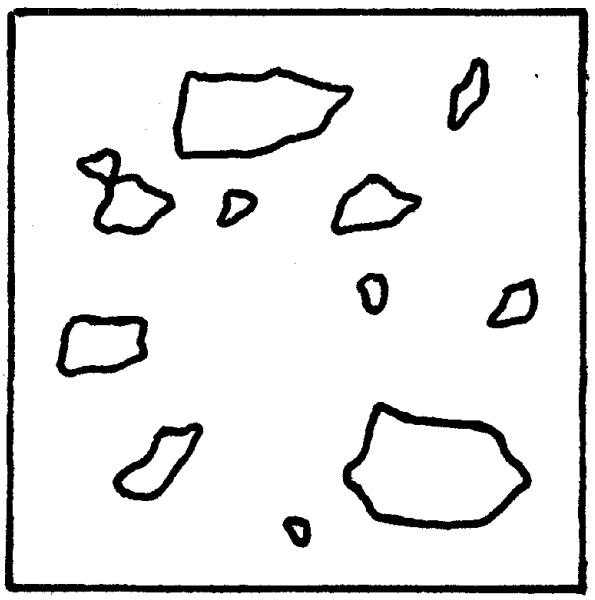

1200X
Silica Flour

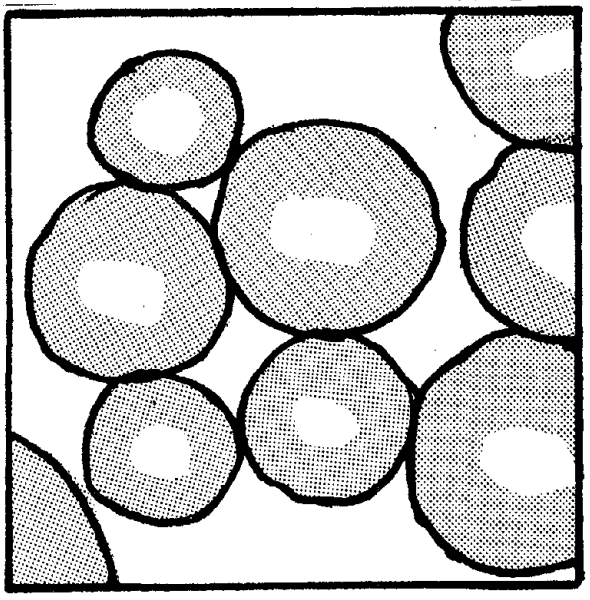

100X
40 to 60 Mesh
.250 - .450 mm
Glass Beads

FIGURE 10. COMPARISON OF GEOMETRIC SHAPE OF FILLER PARTICLES.

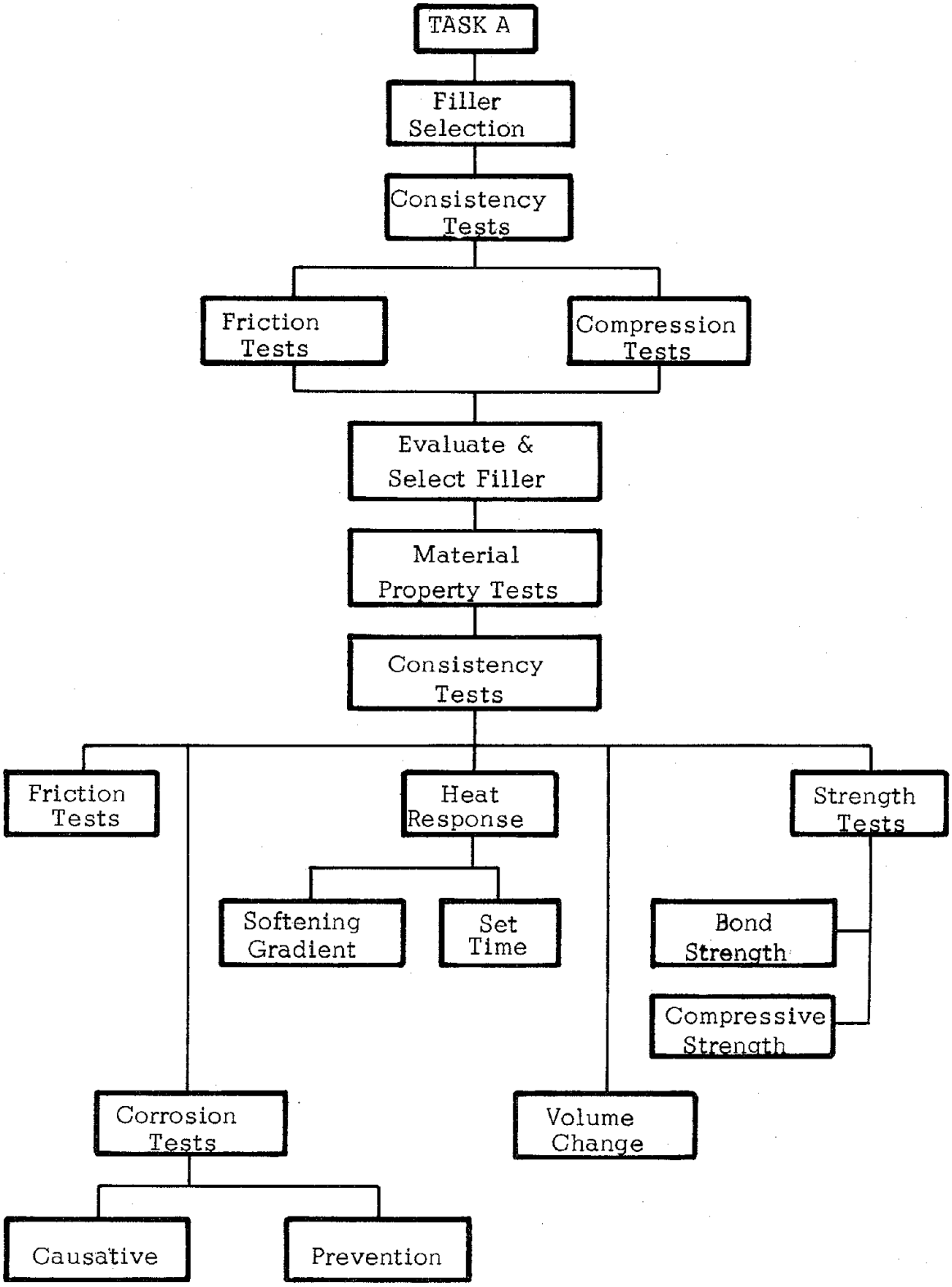

FIGURE 11. FILLER SELECTION AND EVALUATION FLOW CHART.

TABLE 1. FILLER SELECTION TEST RESULTS.

	Fly Ash	Silica Flour	Glass Beads
Specific Gravity	2.65	2.66	2.49
Sieve Analysis	91.1% Passing # 325 Sieve	75.3% Passing #325 Sieve	98.9% Retained #60 Sieve
Consistency [1]			
Brookfield Viscosity Spindel #2 - 2 rpm (Centipoise)	50% HC-1 7,620	50% HC-1 7,840	50% HC-1 7,400
Compressive Strength (psi) [2,3]			
24 hours	- 0 -	18,000	17,000
72 hours	- 0 -	18,000	17,500
Coefficient of Friction [4]	50% HC-1	50% HC-1	50% HC-1
Static	0.90	0.92	0.87
Kinetic	0.80	0.80	0.75

1. Heat Cure #1 (Quadrant Chemical C2057M) epoxy was chosen for the filler selection tests.

2. HC-1 could not be molded properly in standard cube molds. The test specimens were prepared using 1-inch I.D. glass cylinders.

3. The HC-1 and Fly Ash mixture did not cure hard after mixing and heating for one hour at 325°F.(163°C)

4. A 50-milligram film of each item was applied to a glass plate and the coefficient of friction was determined using a 100 gram flat steel bar. The determination of relative friction coefficients was the object of the test.

1 psi = 6.895×10^3 paschal 1 in. = 25.4 mm

termed by the supplier, was substituted for the fly ash when the testing laboratory found that the fly ash epoxy mixtures would not set up for the compression tests.

On the basis of the lower viscosity and friction coefficients for the glass beads, they were chosen for the filler for the friction tests in the concrete blocks.

3) Friction Tests.

a) Results. For consistency, the one-to-one mix ratio used by the testing laboratory was also used for the cement block friction tests. Tendons were coated with the different mixtures and then stressed to a 30 kip (1.334×10^5 Newton) load. From the recordings, the friction loss across each tendon was noted and an average of the losses taken for each set of conduits. In three of the tests, five weight percent of filler was placed by an equal weight of powdered graphite for comparison. Table 2 lists the results of these tests and the epoxies tested.

Comparing the results for the losses obtained from the epoxies against the loss obtained for the bare tendon shows that the epoxy-filler combinations afforded no improvement over the bare tendon friction losses. Presumably, the high viscosity of the mixtures had the greater adverse affects. It may also be noted that the graphite added did lower the losses, though only slightly.

TABLE 2. RESULTS OF FRICTION TESTS OF EPOXY FILLER COMBINATIONS.

Grouts	Friction Loss (lbs)
TP-1 with Filler	7250
TP-1 with Filler and Graphite	7150
TP-2 with Filler	8330
TP-2 with Filler and Graphite	8170
HC-1 with Filler	7080
HC-1 with Filler and Graphite	6750
HC-1 No Filler	7000
HC-1 No Filler with Graphite	6250
HC-2 Special Blend	6250
* Bare Tendon in Rigid Conduit	6000
* Bare Tendon in Flexible Conduit	6120

TP-1 = Nicklepoxy Concrete Injection Resin (product #3)

TP-2 = Shell Epon 828.

HC-1 = Quadrant Chemical C-2057M.

HC-2 = Quadrant Chemical CQL-185-112.

HC-3 = Thermoset DC-725.

* Bare tendon in rigid and flexible conduit gave the lowest friction losses.

1 lbf = 4.448 Newton

It was thought at first that the large size of the glass beads (#60 sieve), coupled with the possibility that they were crushing under the normal force loads, caused the higher friction losses. Two supplementary tests were then performed using the lowest viscosity epoxy (HC-1) with no filler. No decrease in friction losses were obtained and, except for the HC-2 test, further testing planned with the epoxies, including the laboratory tests, were discontinued.

b) Problems. HC-2 was a special blend supplied by a local chemical company. It was mixed with approximately 40 percent by weight of #325 (or better) mesh silica flour and a thixotropic additive. Unfortunately, by the time of testing, and partially due to the lack of air conditioning during part of the shelf time of the epoxies, both the HC-2 and HC-3 had begun to thicken and set. Because of this, the HC-3 was set aside and only one test was made with the HC-2. The consistency of the HC-2 was like taffy and very hard to apply to the tendon and to then install the tendon in the conduit. The HC-2 gave a friction loss equal to that given by the least viscous epoxy with no filler. Considering the result of the single test with HC-2, in the light of the consistency of the epoxy when tested, this particular epoxy-filler combination is worthy of consideration for future tests in the area of cement grouts.

4) Setting Heat Cure Epoxy Grouts

a) Initial Feasibility Tests. As previously mentioned and as shown in Figure 12, tests conducted with an AC arc welder showed that

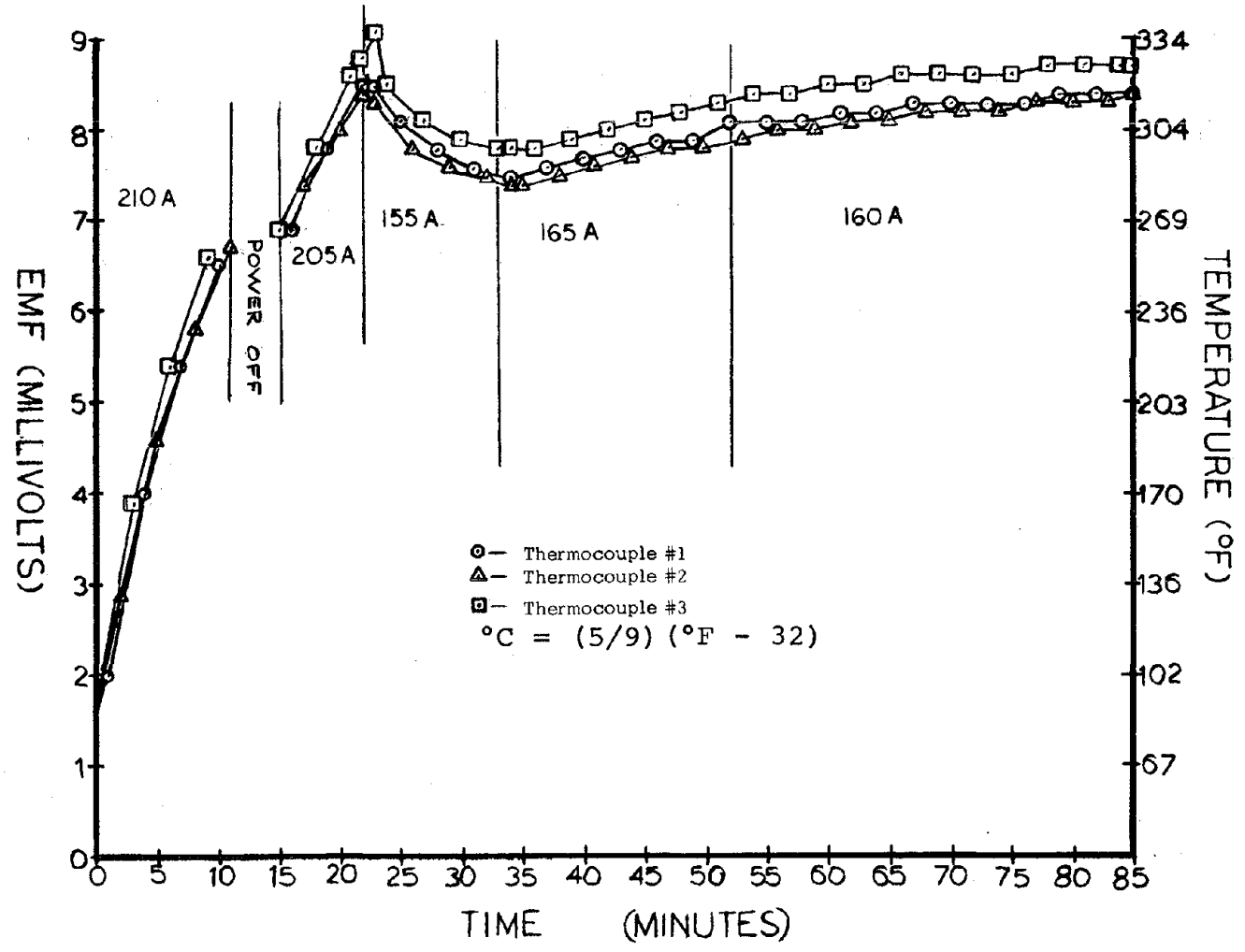

FIGURE 12. STRAND TEMPERATURE VERSUS HEATING TIME - 20-FOOT (6.1 METER) TENDON IN SAND ENVELOPE.

a uniform temperature of 300° - 330° F (149° - 166° C) could be maintained for one hour. There were, however, some conflicting results during the tests. The first tests were run using a 9-foot (2.7 meter) tendon inserted into a test block. A digital voltmeter was used to measure the thermocouple potentials and an ice bath was used for zero reference. The test showed that the three measuring points rose in temperature at a different rate and leveled off and stayed at fairly wide differences in temperature. After a long heating period, the tendon had not reached 300° F (149°C) so the amperage was increased from 200 to 220 amps. The temperatures increased but maintained the wide differences in value. The test is shown in Figure 13. The inset figure (b) of Figure 13 shows the test points on the tendon. The day was sunny and warm.

Another set of tests were run in a different conduit just after a rain. Moisture was removed from the conduit by swabbing the bore with a dry rag. The subsequent tests gave the wide variation in temperatures of Figure 14. The tendon was then moved into open air, supported on polyurethane pads and heated. The tendon increased in temperature uniformly up to 300° F (149° C) as shown in Figure 15.

b) Twenty-foot Tendon. A set of tests was then performed with a 20-foot (6.1 meter) tendon covered with a dry sand envelope. Figure 16 illustrates the test. The test points were covered by polyurethane foam enclosures.

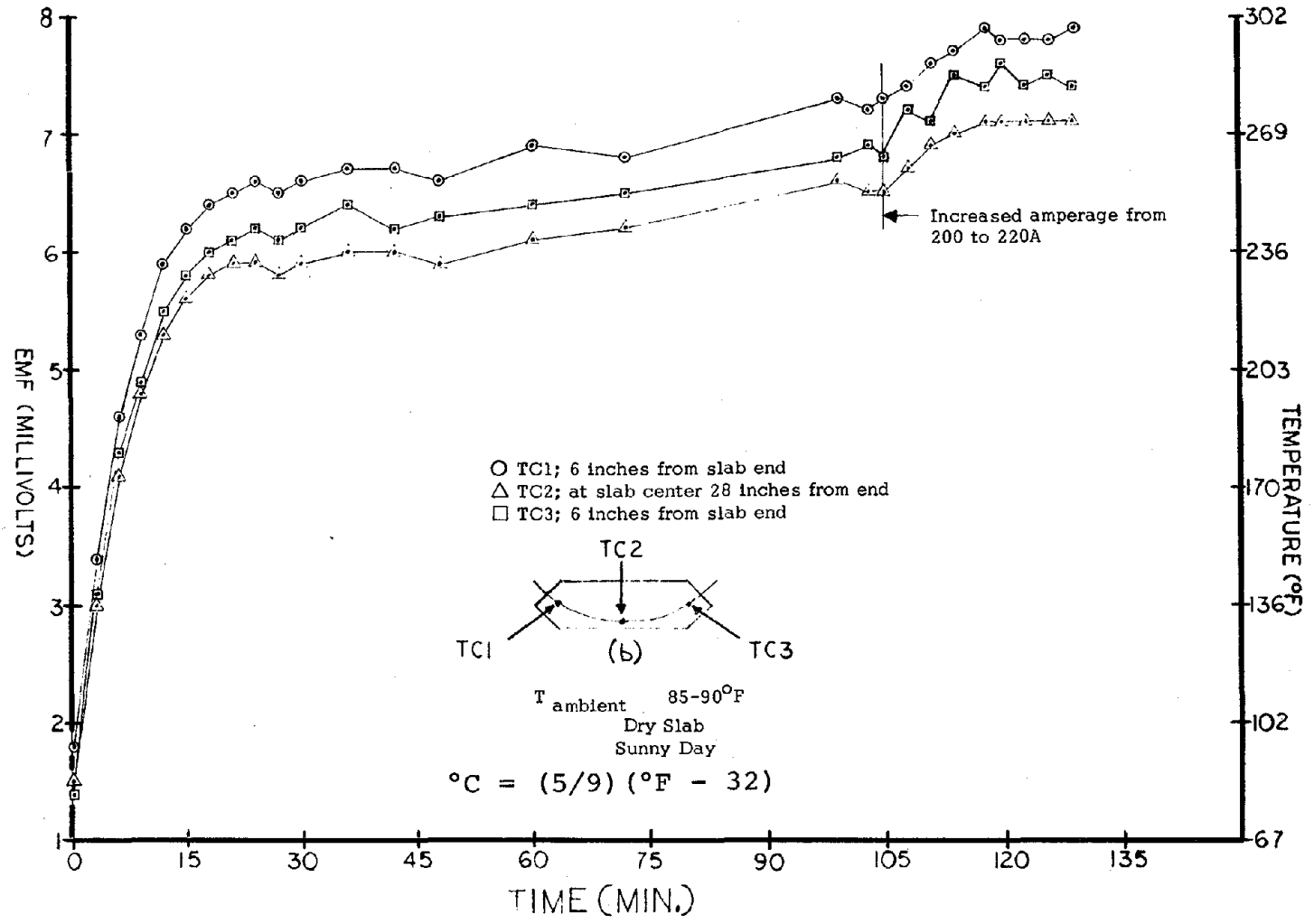

FIGURE 13. STRAND TEMPERATURE VERSUS HEATING TIME - 9-FOOT (2.7 METER) TENDON IN RIGID CONDUIT.

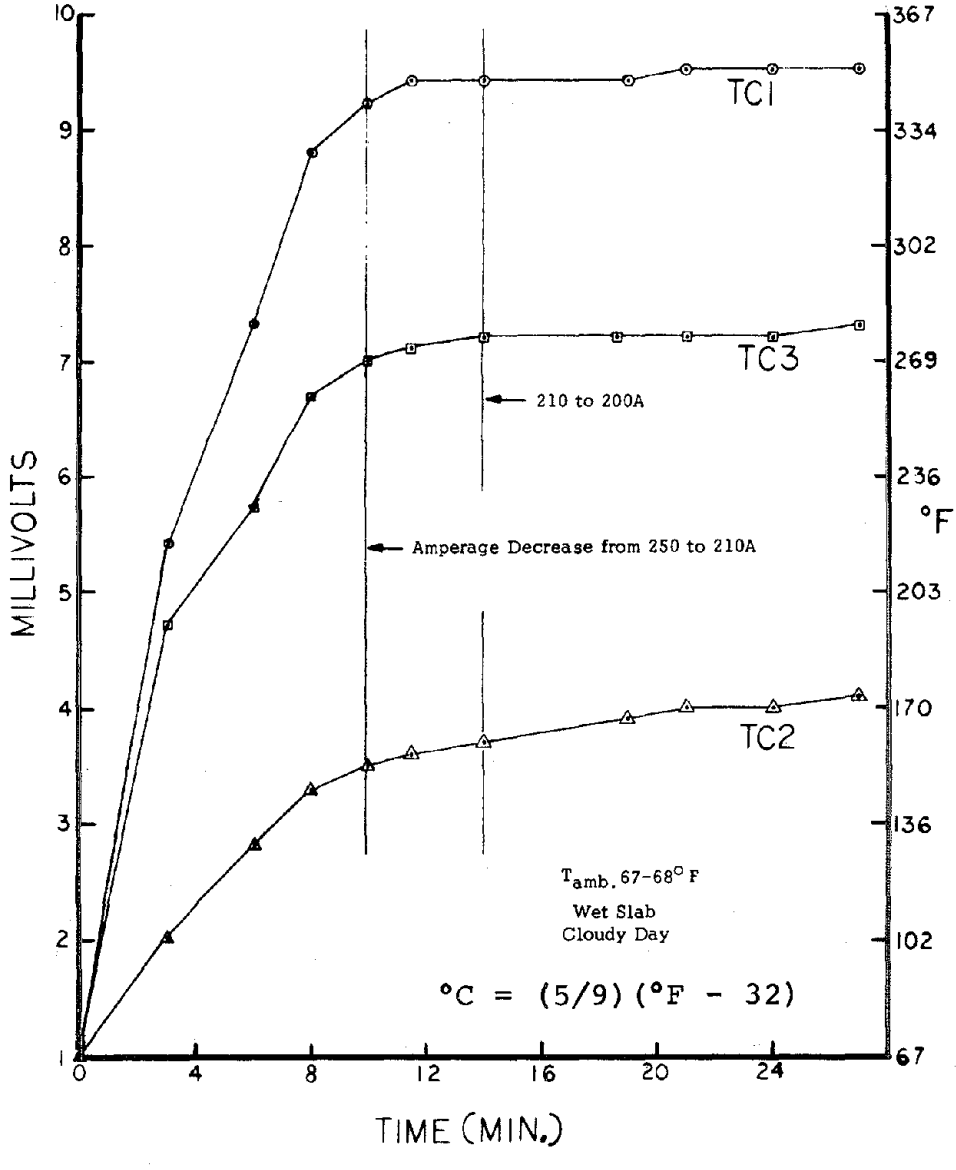

FIGURE 14. STRAND TEMPERATURE VERSUS HEATING TIME - 9-FOOT (2.7 METER) STRAND IN RIGID CONDUIT.

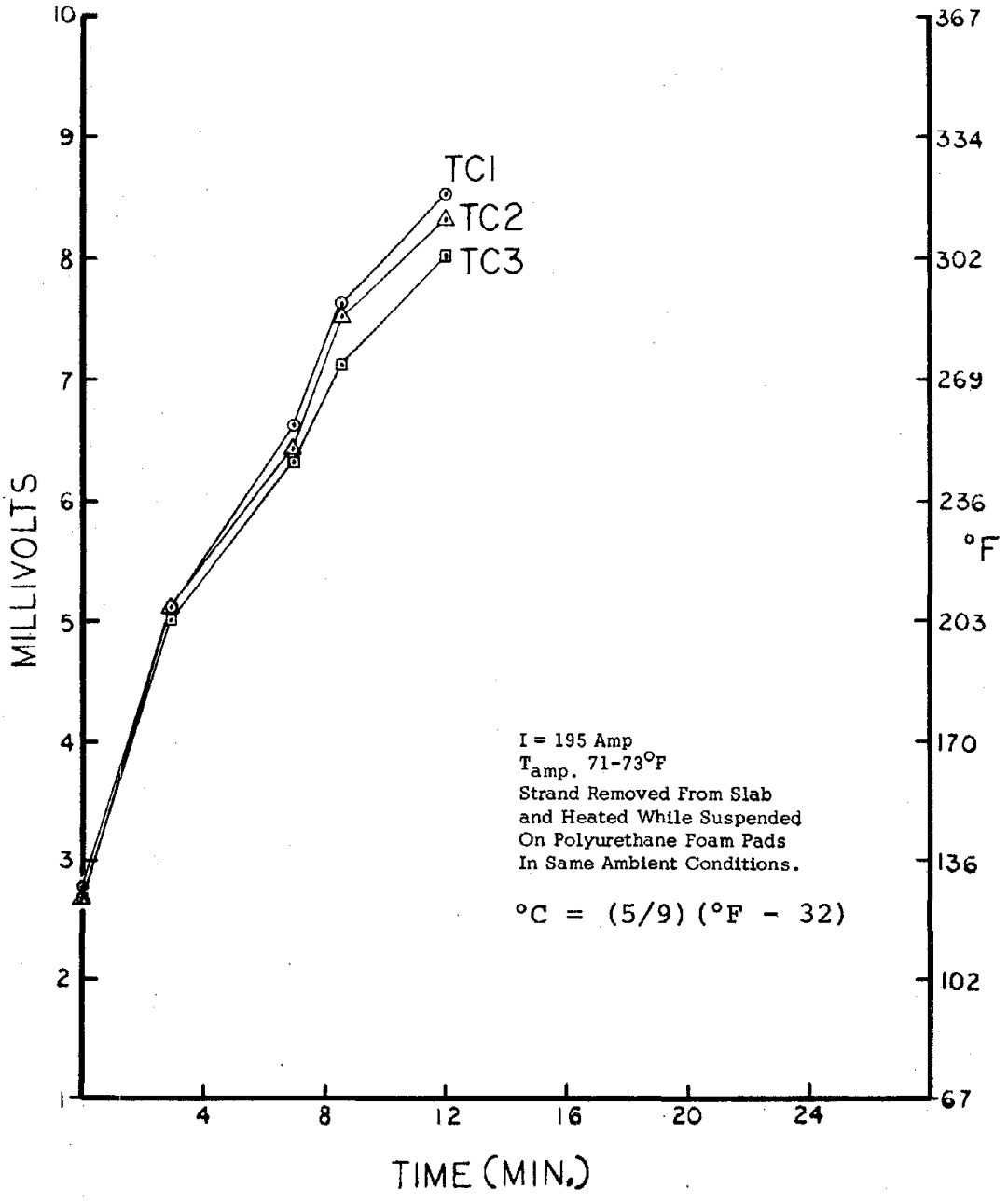

FIGURE 15. STRAND TEMPERATURE VERSUS HEATING TIME - 9-FOOT (2.7 METER) TENDON OUT OF CONDUIT.

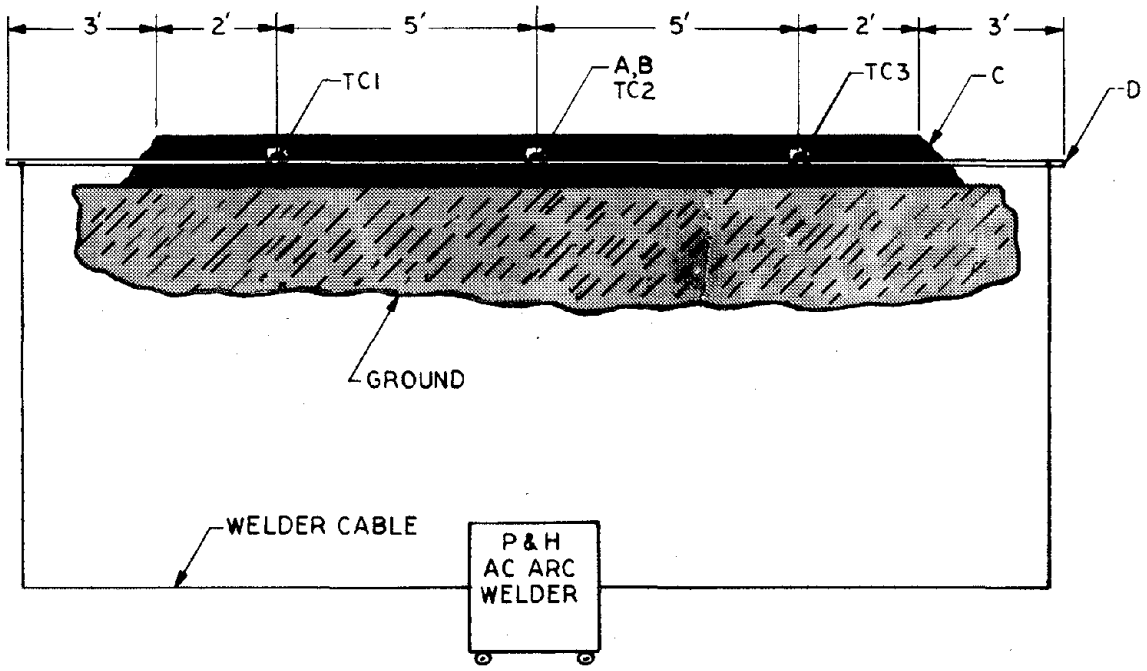

A-POLYURETHANE FOAM ENCLOSURE 1-1/2" SQ.
B-TC1,TC2,TC3,THERMOCOUPLE CONNECTION POINTS
C-DRY SAND ENVELOPE 2" THICK
D-7 WIRE STRAND 20' LONG

1" = 25.4 mm

1' = 304.8 mm

FIGURE 16. 20-FOOT (6.1 METER) STRAND IN DRY SAND ENVELOPE.

The sand acted as a rough simulation of a grout around the tendons. It was expected from the previous tests that the thermal energy would dissipate into the sand and nonuniform heating would result. This was not the case, however, as the tendon heated uniformly as shown in Figure 12.

c) Ten-foot Beams. Two 10-foot (3 meter) concrete beams were then constructed, as illustrated in Figure 17, which would allow placement indoors under controlled conditions. The ultimate purpose of the test was to set a heat cure epoxy pumped into the conduits. First, dry heating tests were run to make sure the tendon would heat uniformly. The outside surfaces of the beams were also monitored by thermocouples to check thermal gradients in the beam induced by high dissipation rates. In other tests, water was poured on the beams and the beams were covered with moist towels to try to induce thermal dissipation through the cement.

In all the tests up to the point of grout setting, the tendons heated uniformly over the 10-foot (3 meter) length. Figure 18 shows the result of a wet beam test which is typical of all the tests. It is possible that the beams were not sufficiently wet to cause variations in temperature such as those of Figure 12.

Grout setting was not carried out because of the results of the friction tests. Instead, efforts were turned back again to the impact studies.

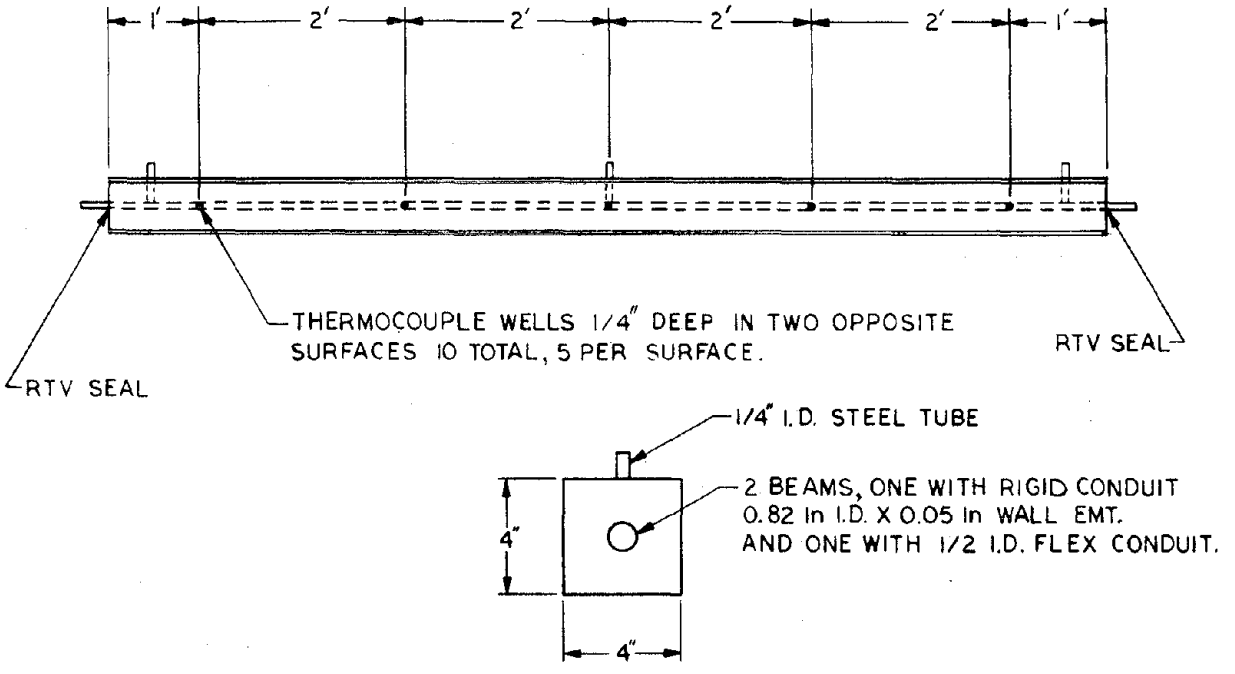

1" = 24.5 mm

1' = 304.8 mm

FIGURE 17. 10-FOOT (3 METER) BEAMS FOR TENDON HEATING TESTS.

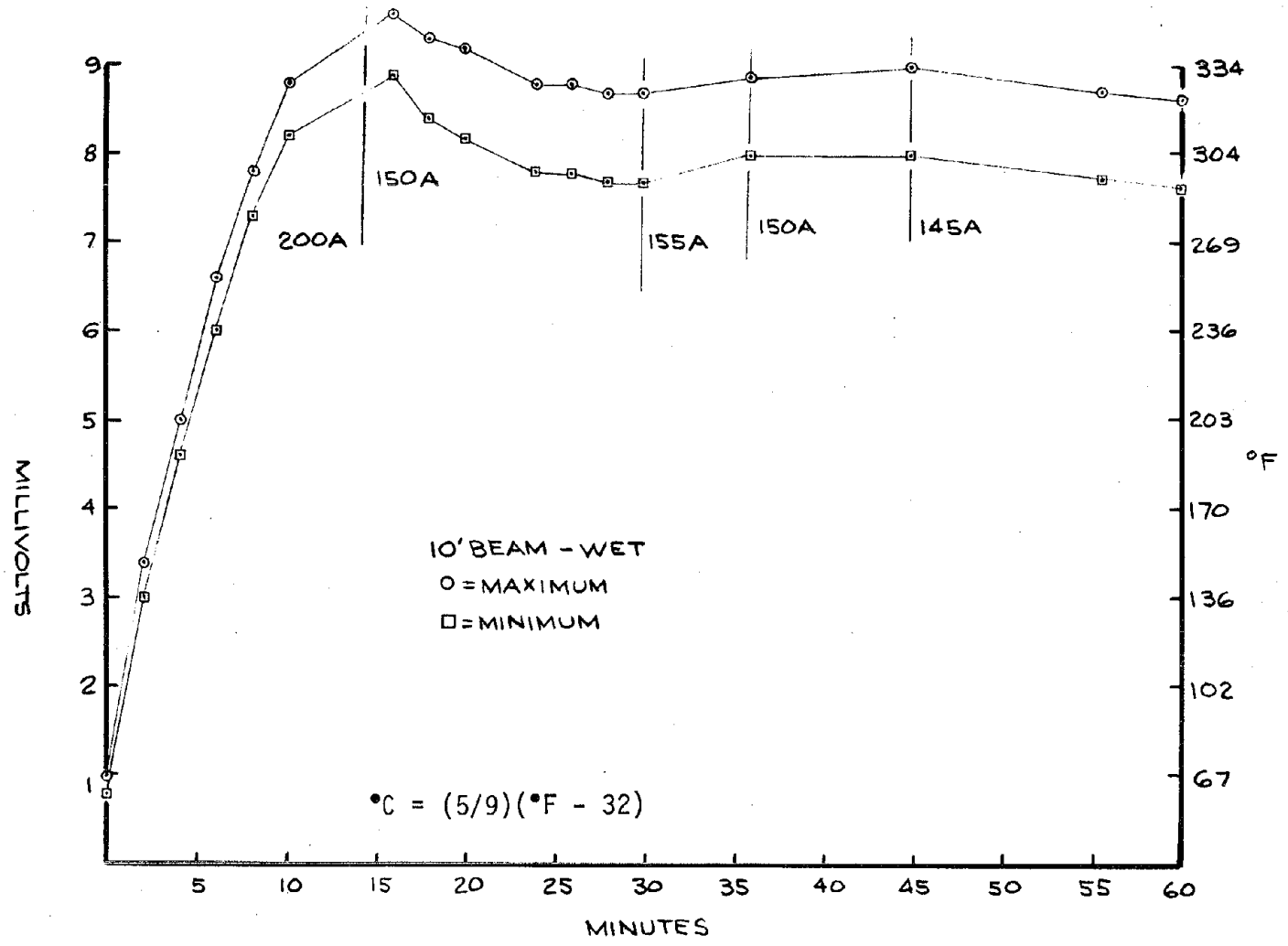

FIGURE 18. STRAND TEMPERATURE VERSUS HEATING TIME - FOR TENDON IN 10-FOOT (3 METER) BEAM IN RIGID CONDUIT.

C. Pneumatic Impact System

A Martin PV-3 impact vibrator was modified to perform purely as an impactor in an effort to generate sharp release pulses for the friction reduction tests. A timer and pneumatic control valve were employed to facilitate control of impact frequencies.

Originally, a factory-built, timed impactor with the same mass piston was to be used, but after a long delay in delivery, inquiry revealed that the impactor ordered was out of production. The PV-3 was settled upon since its dimensions would allow it to easily adapt to the support apparatus constructed for the tests. Figure 19 shows the system ready for testing.

The impact tests were performed at the anchor end of the test blocks. The reasoning was that a release pulse propagating from the anchor end would momentarily lower the normal forces at a point, and as it passed, the local tensile forces would elongate the tendon at the point. The overall result would be an increase in tension all along the tendon as evidenced by a drop in applied tension because of the accumulated elogation. Also, release pulses would not overload the tendon as might occur with increasing applied tension-type pulses.

When the impact system was finally tested, it was found that the limited piston travel would not allow a velocity high enough to achieve a workable range of impact energies. Little data was taken with the system and efforts were turned to the construction of a simple pendulum impacting device.

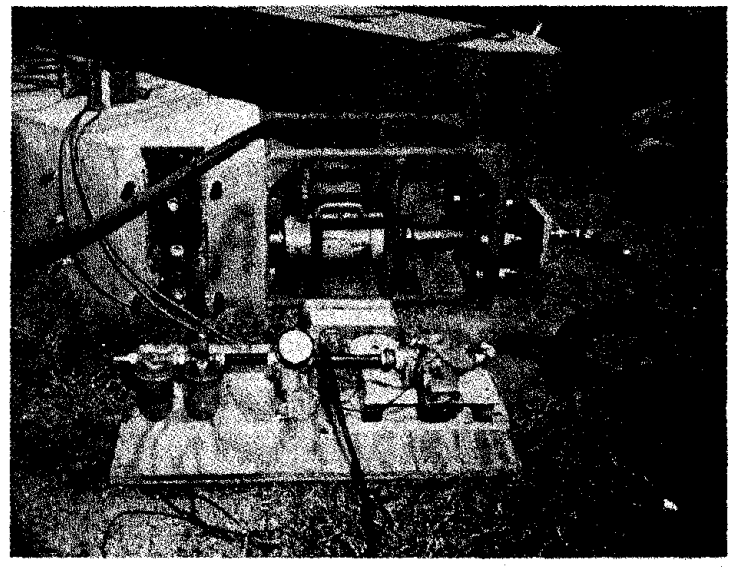

FIGURE 19. PNEUMATIC IMPACT SYSTEM.

D. Impact Pendulum System

1. Description and Procedure. The pendulum system was arranged so that the hammer mass and the pendulum arm length could be varied if necessary. The mass was set at a maximum of six pounds (26.7 Newtons) and the pendulum arm length was adjusted to the maximum obtainable for each tendon. The swing was measured by the use of a degree wheel mounted on the axis of rotation of the pendulum arm. Figures 20 and 21 diagram components of the pendulum apparatus and Figure 22 shows the anchor end ram with load cell and impact plate. Figures 23 (a) and 23 (b) are photos of the test apparatus.

Tests started at a 10^{o} angle and were incremented 10^{o} up to a maximum of 90^{o}. Tests were run at load levels of 10kip (4.448×10^{4} Newton), 20 kip (8.896×10^{4} Newton), and 30 kip (1.334×10^{5} Newton). Each level was impacted at each 10^{o} increment from 10^{o} to 90^{o}. If an anchor tension increase occurred for a particular degree of swing, it was impacted at that angle until no increase occurred. The angle was then incremented and the process repeated.

2. System Advantages and Problems. Advantages of the system were its simplicity and the range of impact amplitudes available. The maximum impact forces at 90^{o} angles were in the 7,000-pound (3.114×10^{4} Newton) range. Impact times ranged from 200 to 500 micro-seconds.

Disadvantages of the system were the inability to vary the impulse duration and the poor repeatability of an impact force at a given pendulum angle. Also, the impact generated free damped oscillation so that the initial pulse effects were clouded by several release-stress cycles.

3. Results and Observations - Static Load Tests. The first tests run were static load tests where the impact magnitude was not incrementally controlled

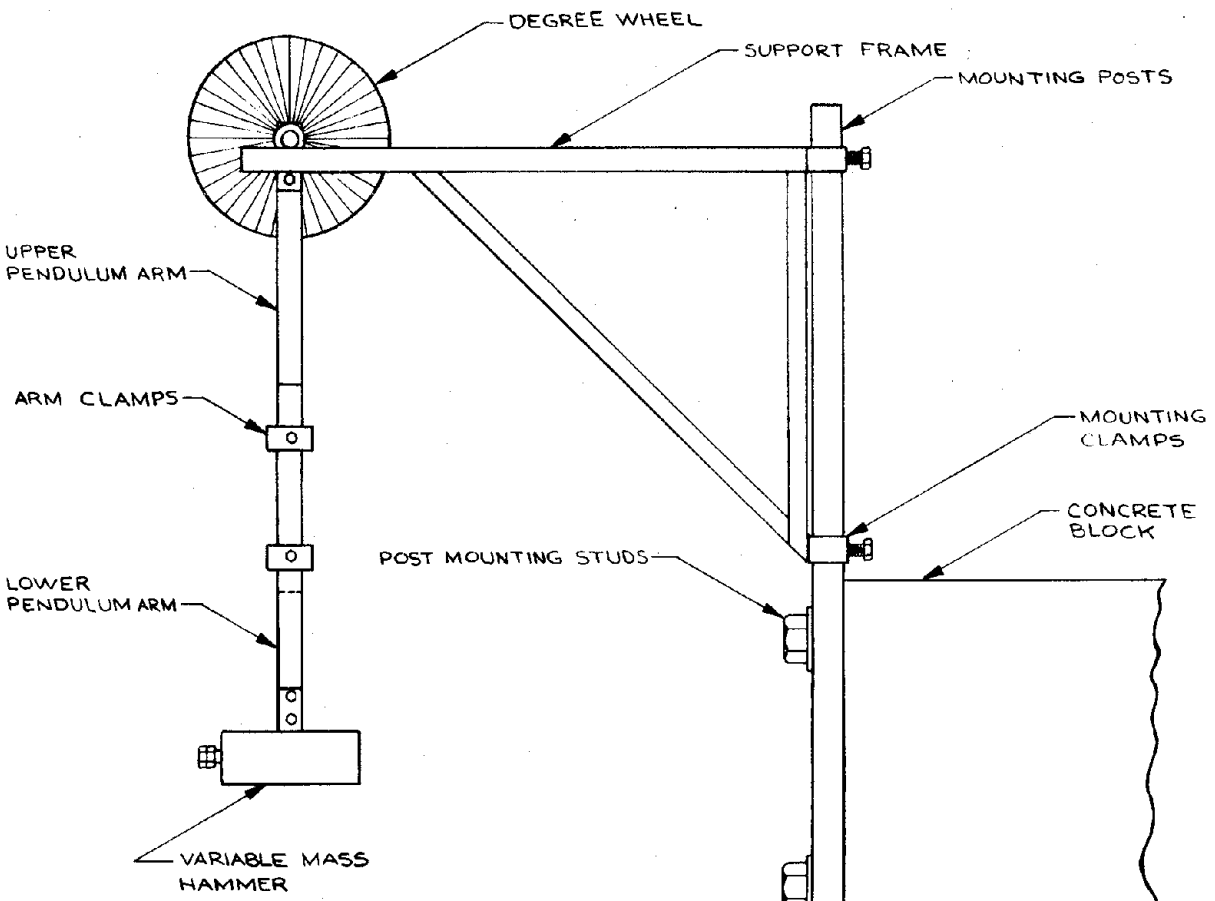

FIGURE 20. IMPACT PENDULUM ASSEMBLY.

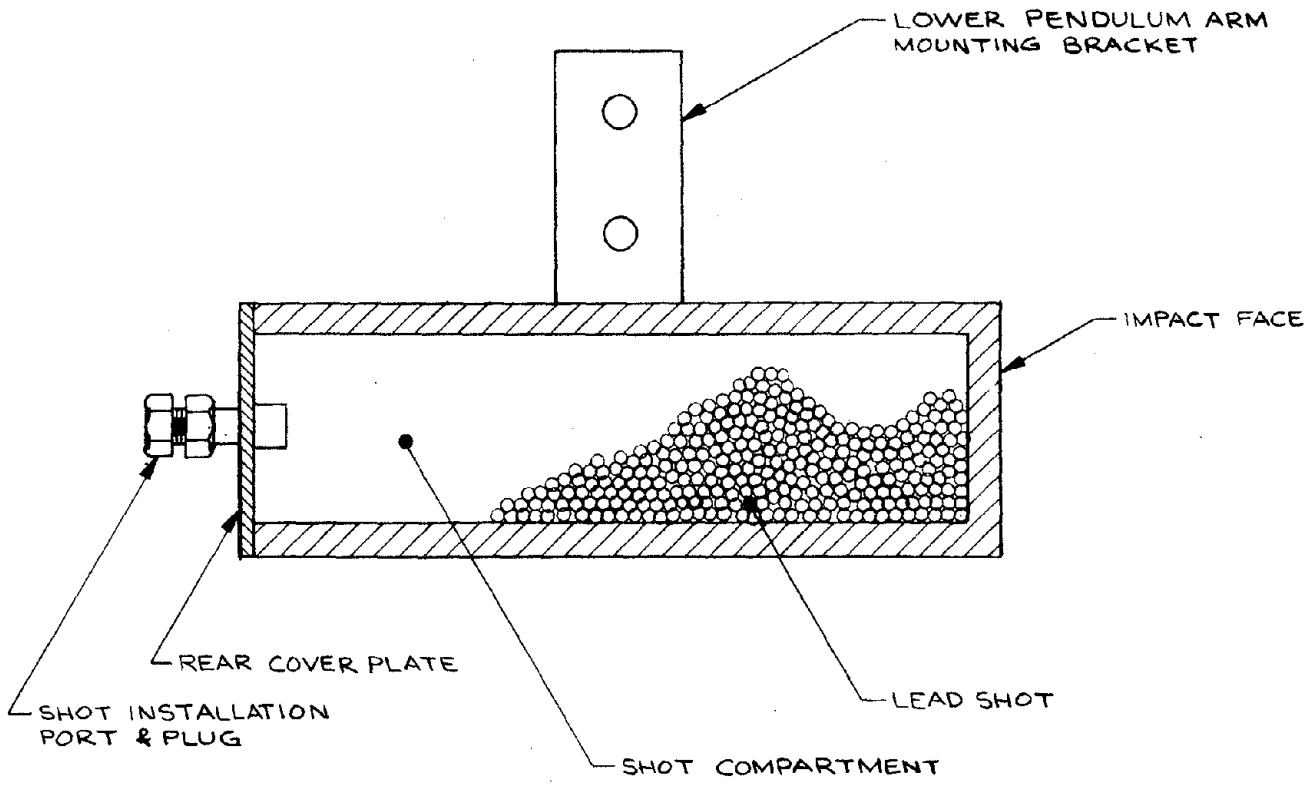

FIGURE 21. VARIABLE MASS HAMMER.

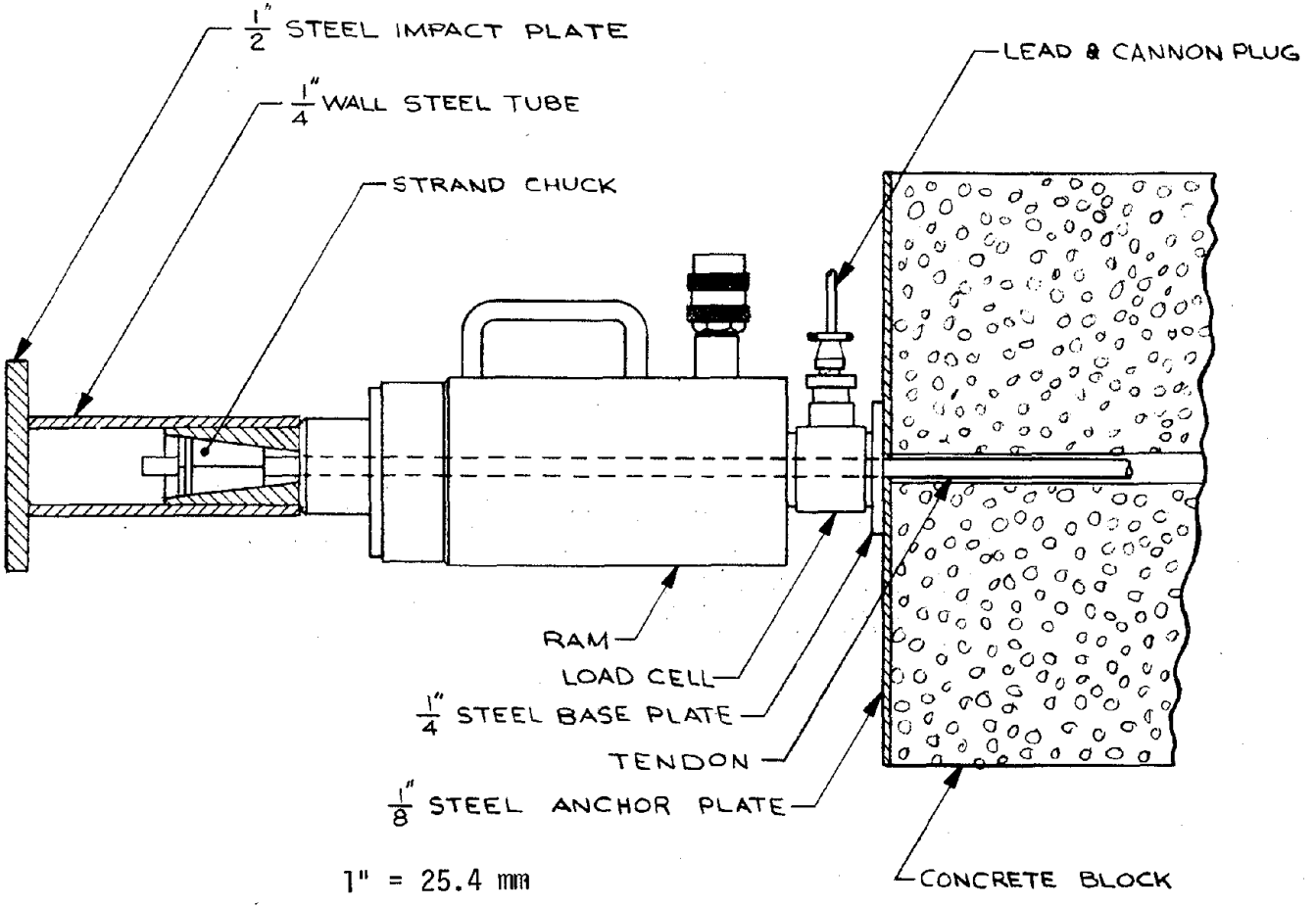

FIGURE 22. ANCHOR END TEST APPARATUS.

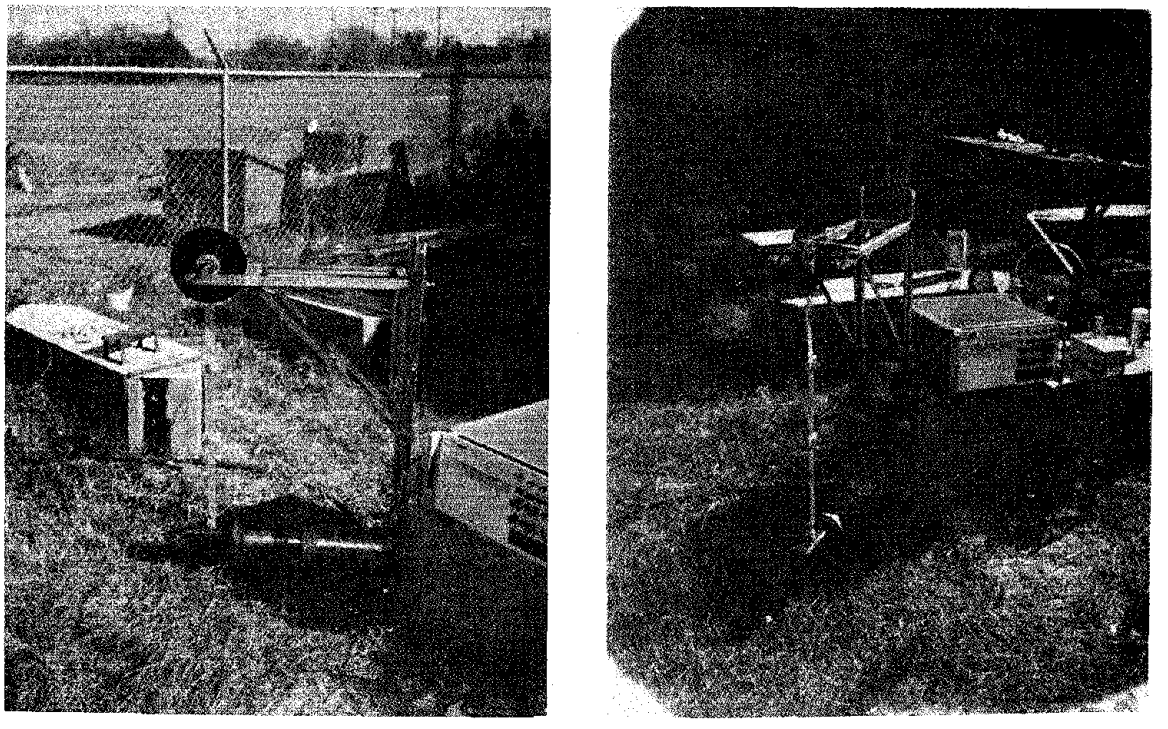

FIGURE 23. IMPACT PENDULUM APPARATUS.

since the maximum anchor end increase was to be studied. The tests are termed "static" in that the applied tension was set and the hydraulics valved off. This was done in order to allow observation of the impact effects at both ends of the tendon. The tendon was impacted until the anchor tension had increased and stopped. Since the applied tension had dropped, the tendon was then retensioned and impacted again to see if the anchor tension would continue to rise. It was found that after a maximum anchor tension was obtained, retensioning and impacting again with the same magnitudes of impact forces resulted in no further increase in anchor tension. However, larger magnitude impact forces would again increase the anchor tension slightly along with corresponding decreases in applied tension.

Tests were performed on one set of three rigid conduits and one set of three flexible conduits. Each tendon was tested at the three load levels of 10 kip (4.448×10^4 Newton), 20 kip (8.896×10^4 Newton), and 30 kip (1.334×10^5 Newton). Each level was impacted until it maximized, beginning with the lowest level and stepping up to the next levels in sequence. The impact magnitude was generally limited to the 10,000-pound (4.448×10^4 Newton) range since appreciable changes in anchor tension, after maximizing, were affected only by sizable increases in impact magnitude. Figure 24 shows a typical recording of a static load test.

After the third level had been maximized, the tendon was detensioned, then retensioned, according to the same procedure except the applied tension was allowed to remain live and return the load to the original level after each impact. This was done in order to determine any advantages offered by either

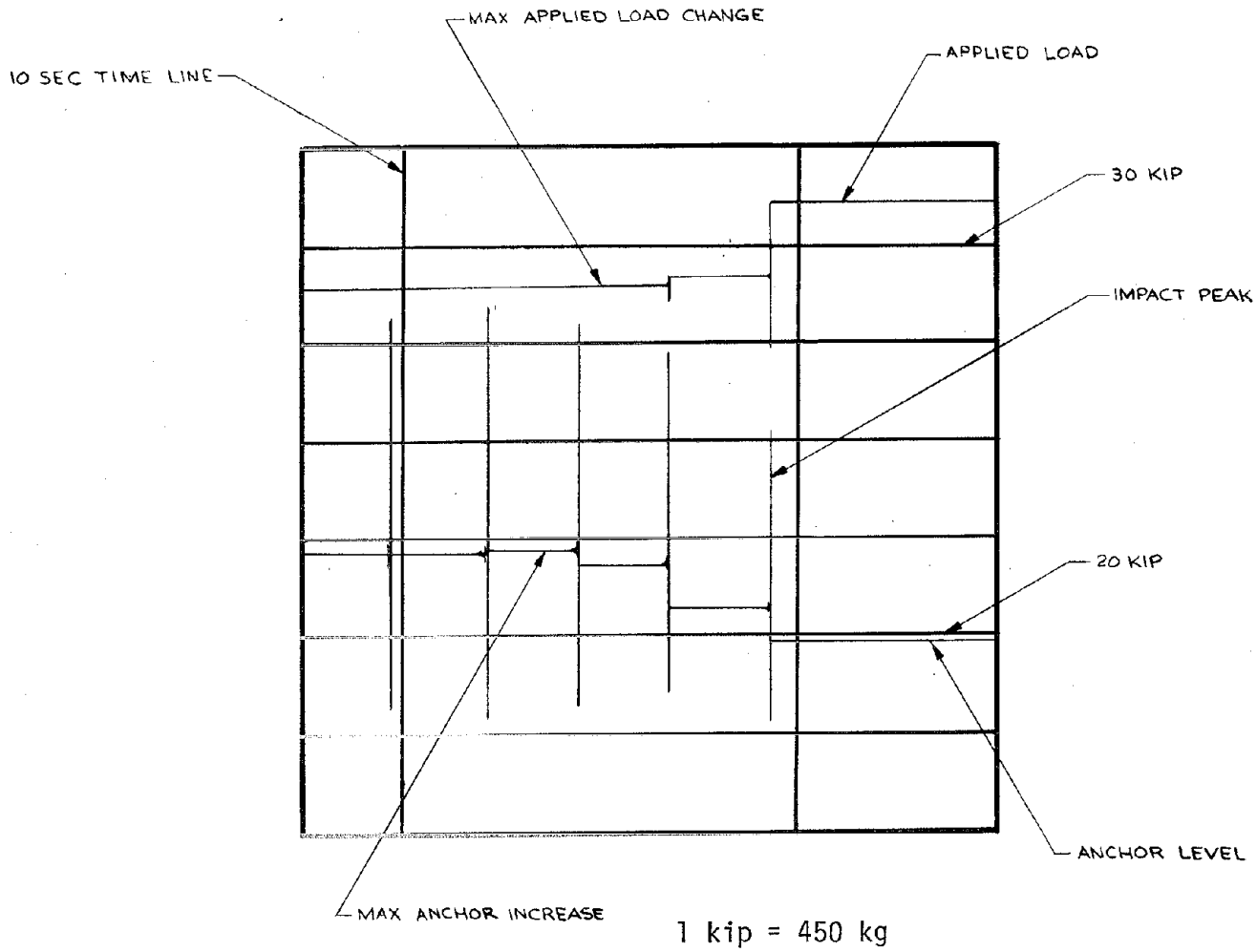

FIGURE 24. TYPICAL STATIC LOAD IMPACT RECORDING.

technique on the final anchor tension as evidenced by the final anchor tension compared to the initial applied tension.

Table 3 lists part of the results showing the initial tensions and the changes in tension for two cases. Case 1 (Anchor 1) is the change in anchor tension when the applied tension had dropped its maximum amount, and the second case (Anchor 2) is the total anchor tension change. The Table also gives the equivalent added applied tension (equivalent force) which would be necessary to increase the anchor tension the Case 1 amount, the maximum impact force applied for the load range under test, and the initial and final ratios of anchor to applied tension. The final anchor to applied tension ratio does not reflect stressing efficiency of the tendon but is only for comparison of the impact effects between tests. It was thought that the flexible conduit might allow a smaller friction loss but no advantages were observed, as the Table shows. The data does exhibit a relationship between the change in applied tension and the equivalent force.

Table 4 compares the results of 30 kip (1.334×10^5 Newton) live load tests with the 30 kip (1.334×10^5 Newton) static load tests. The ratios of final anchor tension to initial applied tension shows that there was no conclusive advantage to either method of raising the anchor tension.

4. Results and Observations - Dynamic Load Tests

a. Impact Characteristics. The second set of impact tests used the impact pendulum with high speed recordings of the impacts. Figure 25 is an example of one recording where the applied tension had dropped.

TABLE 3. APPLIED AND ANCHOR TENSION CHANGE DATA FOR STATIC LOAD IMPACT TESTS.

Initial Tension (lbs)		Level Change (lbs)			Equivalent Force (lbs)	Maximum Impact Force (lbs)	Anchor to Applied Tension Ratio (T_A/T_o)		Conduit F=Flexible R=Rigid
Applied (T_o)	Anchor (T_A)	Applied (ΔT_o)	Anchor 1 (ΔT_A)	Anchor 2 (ΔT_A)	(F_E)	(P_o)	Initial	Final	
11,000	8450	-1500	+1000	+1000	1327	6375	.77	.86	F
20,900	15,163	-1738	+1250	+1462	1658	7838	.73	.80	F
31,850	22,450	-2025	+1463	+2038	1941	8025	.70	.77	F
11,315	8863	- 650	+ 463	+ 526	614	4938	.78	.83	F
21,600	16,088	-1625	+1475	+1563	1957	6688	.74	.82	F
32,250	23,500	-1375	+1213	+1625	1609	7524	.73	.78	F
10,963	8525	- 813	+ 750	+ 813	995	4625	.78	.85	F
21,075	15,550	-1538	+1138	+1250	1510	5563	.74	.80	F
31,438	22,875	-3138	+2650	+3125	3516	9313+	.73	.83	F
10,813	8500	-1150	+ 975	+ 975	1294	6113	.79	.88	R
20,538	16,238	- 913	+ 875	+1300	1161	6563	.79	.85	R
30,313	24,613	- 625	+1025	+1150	1360	6250	.81	.85	R
11,125	8788	- 825	+ 713	+ 838	946	6725	.79	.87	R
21,650	16,625	- 838	+ 538	+ 588	714	7500	.77	.80	R
31,750	23,913	- 750	+ 538	+ .675	714	8000	.75	.77	R
11,150	8350	-1275	+ 650	+1275	862	6125	.75	.86	R
20,863	15,500	-1863	+ 938	+1663	1244	6738	.74	.82	R
31,500	22,500	-2688	+2063	+2438	2737	7050	.71	.79	R

1 lbf = 4.448 Newton

TABLE 4. COMPARISON OF RATIOS OF ANCHOR TO APPLIED TENSION RATIOS FOR STATIC AND LIVE LOAD IMPACT TESTS.

Anchor to Applied Tendon Ratio (T_A/T_o)				Maximum Impact Force (F_E) (lbs)		Conduit F = Flexible R = Rigid
Initial		Final				
Static	Live	Static	Live	Static	Live	
.73	.70	.76	.77	8125	8025	F
.73	.73	.78	.78	7475	7561	F
.73	.73	.82	.83	9000	9313+	F
.73	.71	.81	.77	6938	7050	R
.77	.75	.80	.77	7375	8000	R
.76	.81	.82	.85	5938	6250	R

1 lbf = 4.448 Newton

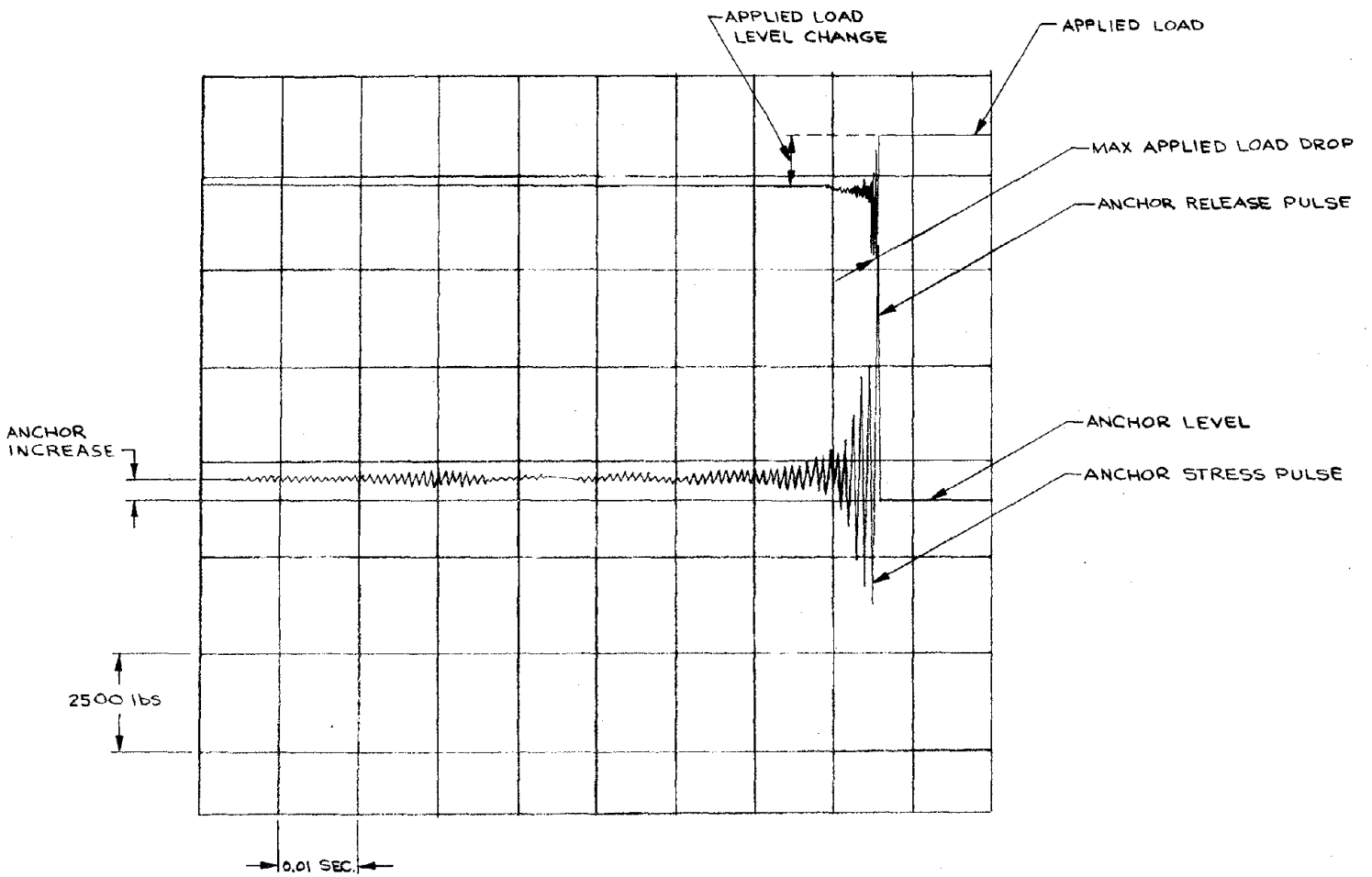

1 lb f = 4.448 Newton

FIGURE 25. HIGH SPEED RECORDING OF IMPACT WITH PENDULUM APPARATUS.

The recordings revealed much about the effects of an impact and the resulting redistribution of forces along the tendon. For example, Figure 25 shows the damped elastic oscillation of the tendon, the large anchor end stressing caused by the reflected stress wave, the shift of the center of oscillation to a new equilibrium position, the dispersing Fourier wave packets, the final anchor tension increase, the decrease in applied tension and high frequency disturbance there, and the final equilibrium level for the applied tension. The high frequency disturbance of the applied tension is probably due to a high velocity "snap" release of tension on that end of the tendon. Since the applied tension was allowed to increase to its original level after each impact the new applied tension in Figure 25 is seen to be gradually increasing. The total time interval of Figure 25 is 0.10 second.

Tables 5 and 6 list the impact data for the maximums of each degree increment for two tests on bare tendons in rigid conduit combinations. Tables 7 through 8 are similar data for bare tendon in flexible conduits. A small amount of cement had leaked into the ends of the flexible conduits and, though they were thought to be cleaned out well, all three conduits exhibited higher than normal friction losses. As can be seen in the Tables, the higher friction dominated the impact effects on the applied load end of the tendons.

The Tables exhibit three forms of final equilibrium conditions after an impact. First, there may be a decrease in the anchor tension with no change in the applied tension as shown in Figure 26 (a). Second, there may be a sizable increase in the anchor tension with no change in applied

TABLE 5. BARE TENDON IN RIGID CONDUIT
(a) LEVEL I - 10 KIP (4.448×10^4 NEWTON)

Pendulum Swing Angle (Degrees)	Impact Force (P_o) (Pounds)	Anchor Level Change (ΔT_A) (Pounds)	Maximum Applied Load Drop (P_L) (Pounds)	Applied Load Level Change (ΔT_A) (Pounds)
10	900	- 25	0	0
20	1738	- 25	0	0
30	2913	+ 75	0	0
40	3438	+ 50	0	0
50	4075	+163	0	0
60	4713	+175	-125	- 75
70	5375	+200	-688	-175
80	5113	+ 62	0	0
90	6313	+100	0	0

1 lbf = 4.448 Newton

TABLE 5. BARE TENDON IN RIGID CONDUIT (Continued)
(b) LEVEL II - 20 KIP (8.896×10^4 NEWTON)

Pendulum Swing Angle (Degrees)	Impact Force (P_o) (Pounds)	Anchor Level Change (ΔT_A) (Pounds)	Maximum Applied Load Drop (P_L) (Pounds)	Applied Load Level Change (ΔT_A) (Pounds)
10	850	- 12	0	0
20	1925	- 12	0	0
30	2538	- 63	0	0
40	3538	0	0	0
50	4000	- 25	0	0
60	4913	- 38	0	0
70	6463	+438	-1788	-625
80	5750	+125	0	0
90	7625	+475	-2125	-725

1 lbf = 4.448 Newton

TABLE 5. BARE TENDON IN RIGID CONDUIT (Continued)
(c) LEVEL III - 30 KIP (1.334×10^5 NEWTON)

Pendulum Swing Angle (Degrees)	Impact Force (P_o) (Pounds)	Anchor Level Change (ΔT_A) (Pounds)	Maximum Applied Load Drop (P_L) (Pounds)	Applied Load Level Change (ΔT_A) (Pounds)
10	950	- 50	0	0
20	1913	- 75	0	0
30	2725	- 75	0	0
40	3538	0	0	0
50	4138	+100	0	0
60	5438	+350	-1163	- 413
70	6663	+613	-3275	-1287
80	6750	+175	0	0
90	7138	+ 25	0	0

1 lbf = 4.448 Newton

TABLE 6. BARE TENDON IN RIGID CONDUIT
(a) LEVEL I - 10 KIP (4.448×10^4 NEWTON)

Pendulum Swing Angle (Degrees)	Impact Force (P_o) (Pounds)	Anchor Level Change (ΔT_A) (Pounds)	Maximum Applied Load Drop (P_L) (Pounds)	Applied Load Level Change (ΔT_A) (Pounds)
10	688	- 13	0	0
20	1275	0	0	0
30	2725	+125	0	0
40	3063	+125	0	0
50	3850	+200	- 925	-263
60	4875	+275	-1250	-288
70	4775	+ 75	0	0
80	4835	+ 37	0	0
90	6888	+162	-1188	-325

1 lbf = 4.448 Newton

TABLE 6. BARE TENDON IN RIGID CONDUIT (Continued)
(b) LEVEL II - 20 KIP (8.896 X 10^4 NEWTON)

Pendulum Swing Angle (Degrees)	Impact Force (P_o) (Pounds)	Anchor Level Change (ΔT_A) (Pounds)	Maximum Applied Load Drop (P_L) (Pounds)	Applied Load Level Change (ΔT_A) (Pounds)
10	900	- 13	0	0
20	1613	- 25	0	0
30	3025	+ 75	0	0
40	3375	+ 62	0	0
50	4050	+ 62	0	0
60	3713	+ 13	0	0
70	4563	+ 12	0	0
80	6388	+575	-2675	0
90	6513	+100	0	0

1 lbf = 4.448 Newton

TABLE 6. BARE TENDON IN RIGID CONDUIT (Continued)
(c) LEVEL III - 30 KIP (1.334 X 10^5 NEWTON)

Pendulum Swing Angle (Degrees)	Impact Force (P_o) (Pounds)	Anchor Level Change (ΔT_A) (Pounds)	Maximum Applied Load Drop (P_L) (Pounds)	Applied Load Level Change (ΔT_A) (Pounds)
10	888	- 25	0	0
20	1650	- 50	0	0
30	2663	- 50	0	0
40	3600	+ 88	0	0
50	4188	+100	0	0
60	4588	+ 63	0	0
70	4600	0	0	0
80	5700	+413	-2638	-1000
90	5850	+ 88	0	0

1 lbf = 4.448 Newton

TABLE 7. BARE TENDON IN FLEXIBLE CONDUIT
(a) LEVEL I - 10 KIP (4.448×10^4 NEWTON)

Pendulum Swing Angle (Degrees)	Impact Force (P_o) (Pounds)	Anchor Level Change (ΔT_A) (Pounds)	Maximum Applied Load Drop (P_L) (Pounds)	Applied Load Level Change (ΔT_A) (Pounds)
10	775	- 25	0	0
20*	-	-	-	-
30	2075	- 37	0	0
40*	-	-	-	-
50	3375	+112	0	0
60	4050	+200	0	0
70	3850	+ 63	0	0
80	4525	+200	0	0
90	4638	+ 62	0	0

* Record timing error - missed peak.

1 lbf = 4.448 Newton

TABLE 7. BARE TENDON IN FLEXIBLE CONDUIT (Continued)
(b) LEVEL II - 20 KIP (8.896×10^4 NEWTON)

Pendulum Swing Angle (Degrees)	Impact Force (P_o) (Pounds)	Anchor Level Change (ΔT_A) (Pounds)	Maximum Applied Load Drop (P_L) (Pounds)	Applied Load Level Change (ΔT_A) (Pounds)
10	800	- 25	0	0
20	1475	-100	0	0
30	2163	-150	0	0
40	2275	-162	0	0
50	3163	-125	0	0
60	3863	- 50	0	0
70	4725	+175	0	0
80	5638	+263	0	0
90	6000	+163	0	0

1 lbf = 4.448 Newton

TABLE 7. BARE TENDON IN FLEXIBLE CONDUIT (Continued)
(c) LEVEL III - 30 KIP (1.334×10^5 NEWTON)

Pendulum Swing Angle (Degrees)	Impact Force (P_o) (Pounds)	Anchor Level Change (ΔT_A) (Pounds)	Maximum Applied Load Drop (P_L) (Pounds)	Applied Load Level Change (ΔT_A) (Pounds)
10	850	- 37	0	0
20	1438	- 63	0	0
30	2200	-133	0	0
40	3275	-133	0	0
50	3950	-100	0	0
60	4250	- 62	0	0
70	5438	+ 75	0	0
80	5925	+150	0	0
90	6125	+187	0	0

1 lbf = 4.448 Newton

TABLE 8. BARE TENDON IN RIGID CONDUIT
(a) LEVEL I - 10 KIP (4.448×10^4 NEWTON)

Pendulum Swing Angle (Degrees)	Impact Force (P_o) (Pounds)	Anchor Level Change (ΔT_A) (Pounds)	Maximum Applied Load Drop (P_L) (Pounds)	Applied Load Level Change (ΔT_A) (Pounds)
10	688	- 25	0	0
20	1125	- 50	0	0
30	1813	- 63	0	0
40	3150	+125	0	0
50	3750	+113	0	0
60	3663	+ 25	0	0
70	4088	+ 87	0	0
80	5438	+ 63	0	0
90	7175	+175	-750	-188

1 lbf = 4.448 Newton

TABLE 8. BARE TENDON IN FLEXIBLE CONDUIT (Continued)
(b) LEVEL II - 20 KIP (8.896×10^4 NEWTON)

Pendulum Swing Angle (Degrees)	Impact Force (P_o) (Pounds)	Anchor Level Change (ΔT_A) (Pounds)	Maximum Applied Load Drop (P_L) (Pounds)	Applied Load Level Change (ΔT_A) (Pounds)
10	900	- 25	0	0
20	1788	- 75	0	0
30	2488	- 50	0	0
40	4288	+100	0	0
50	5075	+138	0	0
60	4275	0	0	0
70	4775	- 12	0	0
80	5825	0	0	0
90	6913	+400	0	0

1 lbf = 4.448 Newton

TABLE 8. BARE TENDON IN FLEXIBLE CONDUIT (Continued)
(c) LEVEL III - 30 KIP (1.334×10^5 NEWTON)

Pendulum Swing Angle (Degree)	Impact Force (P_o) (Pounds)	Anchor Level Change (ΔT_A) (Pounds)	Maximum Applied Load Drop (P_L) (Pounds)	Applied Level Level Change (ΔT_A) (Pounds)
10	838	- 37	0	0
20	1600	- 87	0	0
30	2300	-113	0	0
40	2900	-162	0	0
50	3763	- 13	0	0
60	4875	+ 50	0	0
70	5213	+ 75	0	0
80	6200	+188	0	0
90	7850	+188	0	0

1 lbf = 4.448 Newton

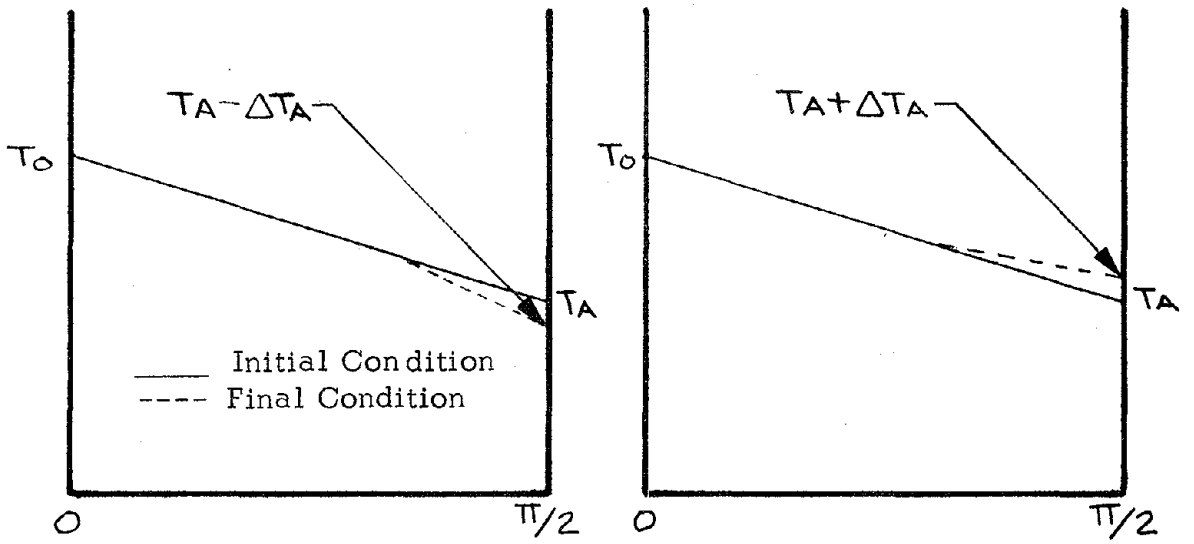

(a) Decrease in Anchor Tension T_A with no change in Applied Tension T_o

(b) Increase in Anchor Tension T_A with no change in Applied Tension T_o

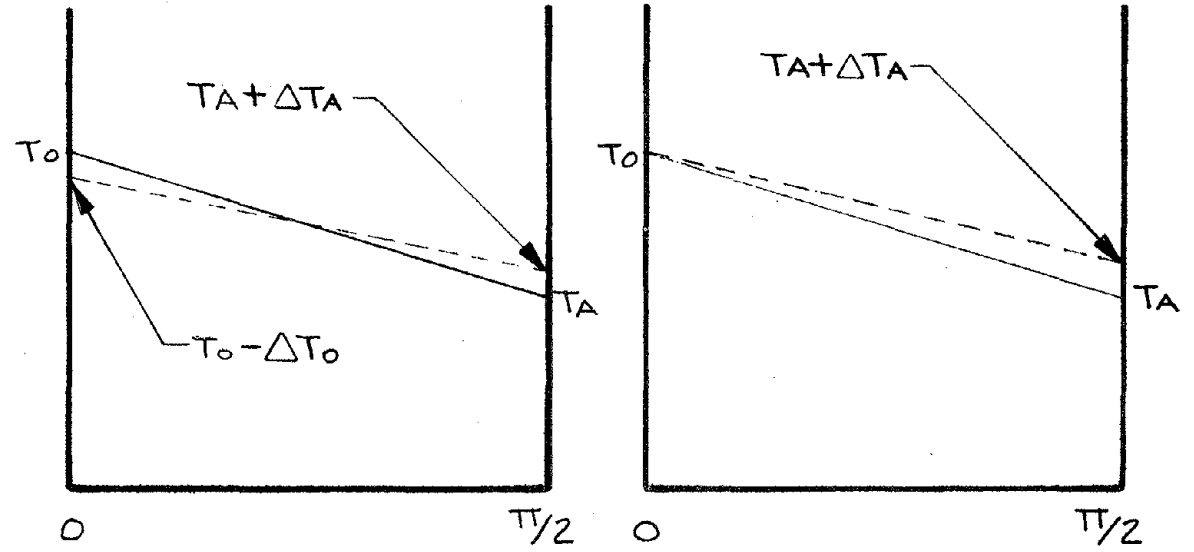

(c) Decrease in Anchor Tension T_A with drop in Applied Tension T_o

(d) Desired effect where Tension increases all along Tendon

FIGURE 26. FORMS OF EQUILIBRIUM CONDITIONS AFTER IMPACT

tension as shown in Figure 26 (b). Third, there may be an increase in anchor tension and a corresponding decrease in tension of the applied load as shown in Figure 26 (c). The desirable impact effect which would allow a uniform increase in tension along the tendon is shown in Figure 26 (d). The tabulated date is indicative of the end conditions only and does not give the actual tension toward the middle of the block. But this data, together with the recordings, such as Figure 25, and some rationale of the mechanics involved allows some assumptions to be made.

b. Mechanics. Earlier in the report, it was mentioned that the reasoning behind the effectiveness of an anchor end impact was that a momentary decrease in the anchor tension also decreases normal forces and thus, frictional resistance along the tendon. When a large enough decrease occurs, the applied tension is then allowed to redistribute along the tendon by a percentage of the magnitude of the drop in friction forces. A large enough release pulse at the anchor end would be one which releases enough tension tied up by frictional forces to first overcome the static friction force and then allow the tension along the tendon to increase proportionately with the released forces. Only a percentage of the total possible increase could be attained since the duration time of the magnitude of the impact force sufficient to allow redistribution of tension is shorter than the duration of the full impact. The extent of redistribution of tension is then indicated by an increase in anchor tension and a decrease in applied tension.

The magnitude of the decrease in applied tension because of redistribution of tension should then fall in the range of the equivalent added applied force necessary to increase the anchor tension the observed amount. Table 3 compares the drop in applied tension with the equivalent force calculated from the Case 1 increases in anchor tensions. Figure 27 is a plot of this data against a theoretical reference line for comparison. The reference line uses the average friction coefficient for the whole group. As can be seen, there seems to be a parallel between the data points and the theoretical line. Figure 28 (a) depicts the final stress distribution under these assumptions. (In the stress diagrams, the curves are nearly linear, so straight line graphs have been used for simplicity.)

After studying the data, along with the high speed recordings of the impacts, it became apparent, for the case where there is a decrease in applied tension, that this did not mean there was an increase in tension all along the tendon, and that a final indicated anchor end increase in tension did not necessarily indicate the actual increase in tension of the anchor end. The anchor increase could actually be greater than the final equilibrium indication since it was possible for the increasing phase of the generated elastic wave to stress the tendon from the anchor direction. Static friction forces would lock in some of the tension, allowing a final anchor end indication somewhat relaxed from the actual tension when the tendon finally settled at its new equilibrium position.

This reasoning may be applied to the first case of Figure 26 where a decrease in anchor tension occurs. Here the release pulse is small

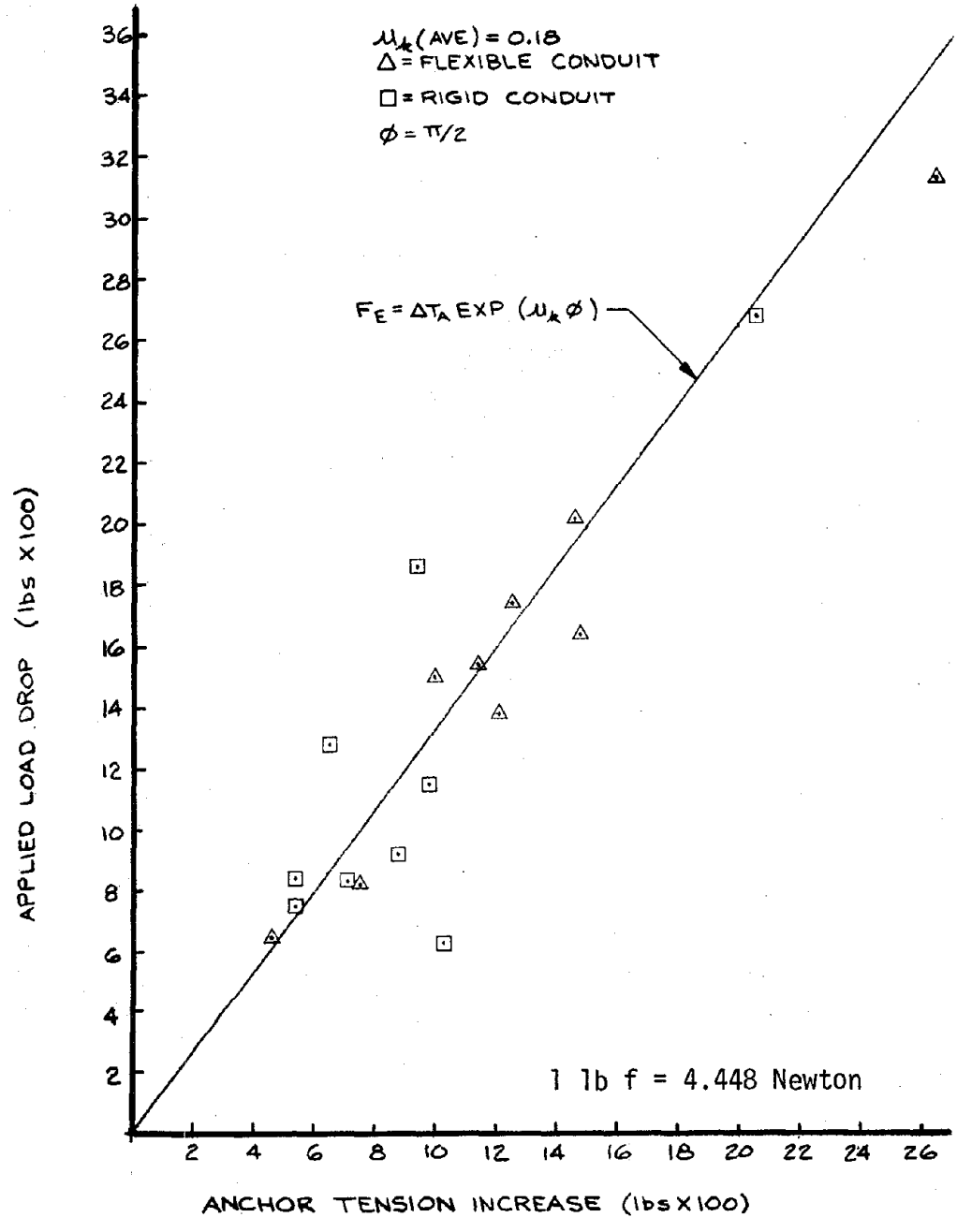

FIGURE 27. APPLIED TENSION DECREASE (ΔT_O) VERSUS ANCHOR TENSION INCREASE (ΔT_A) COMPARED TO PREDICTED EQUIVALENT FORCE, F_E.

enough with respect to the static friction forces so that it is cancelled not far from the anchor end. The increasing tension phase of the elastic wave then stresses the tendon toward the anchor end. It is then possible for increased frictional forces at the anchor end to lock in part of any increase in tension which may occur. Since the friction loss along the tendon near the anchor end also increases with the increase in tension, a negative indication for the anchor tension is obtained after the tendon relaxes to its equilibrium position. Figure 28 (b) shows the stress distribution for this case. (Note that with respect to the shape of the curves, the final elongation of the tendon must be greater than the amount of initial relaxation in order to have a net decrease in tension at the anchor end.)

For the case of Figure 26 (b) where the anchor tension increases, the same effects occur but the release pulse in large enough so that the total relaxation locked in by the friction forces is greater than the elongation of the increasing tension phase of the cycle. The result is an increase in the anchor tension but now, because of the greater amount of relaxation, there is a possible dip in tension where the release pulse was cancelled. This situation is illustrated in Figure 28 (c).

For the case of Figure 26 (d), as was observed earlier in the discussion of the original thoughts on the impact mechanics, only a percentage of the possible increase in anchor tension is possible because of the short duration of the impulse. This gives rise to another observable aspect which is the phase relationship between the magnitudes of the impact

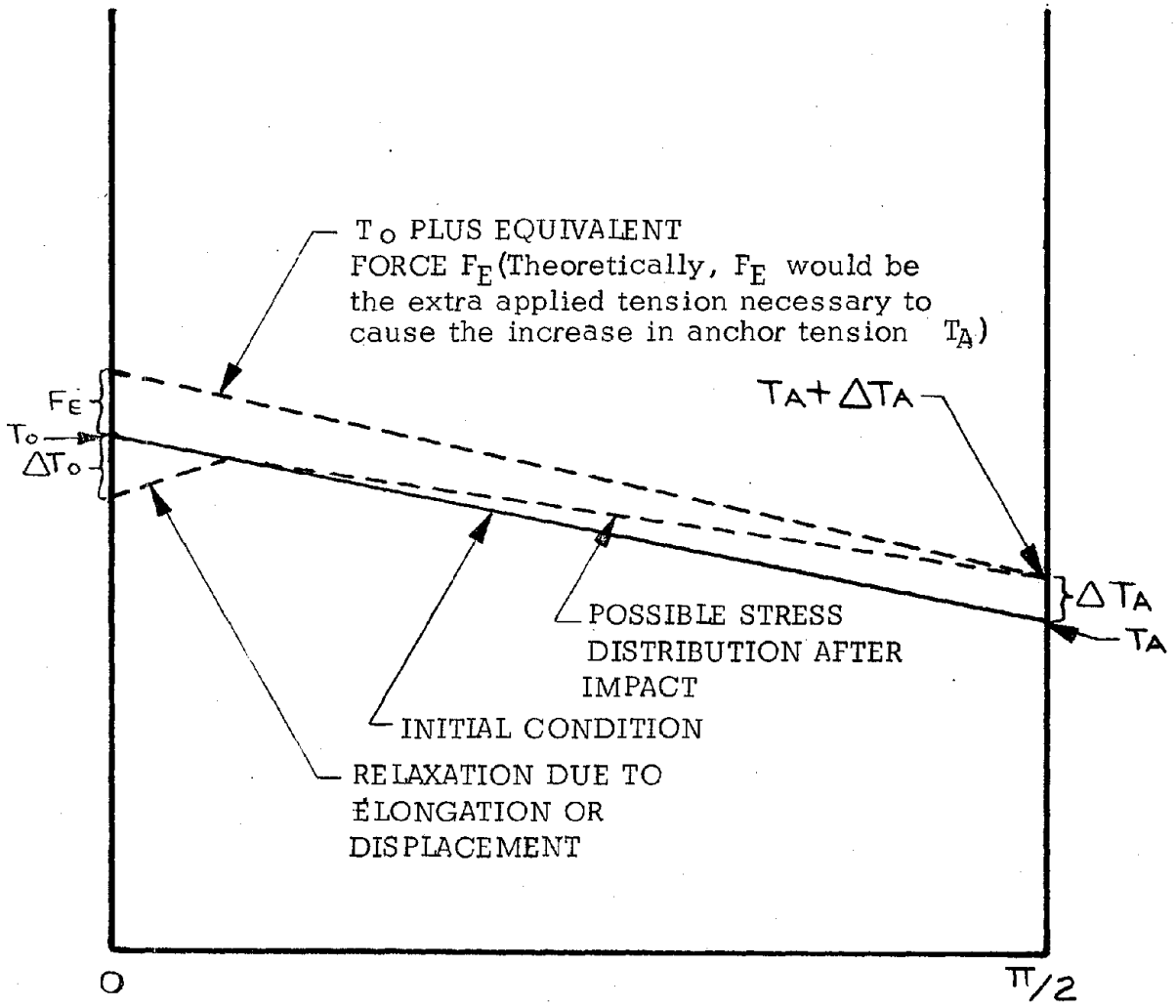

(a) After Impact as Assumed Initially.

FIGURE 28. PROBABLE STRESS DISTRIBUTION ALONG TENDON

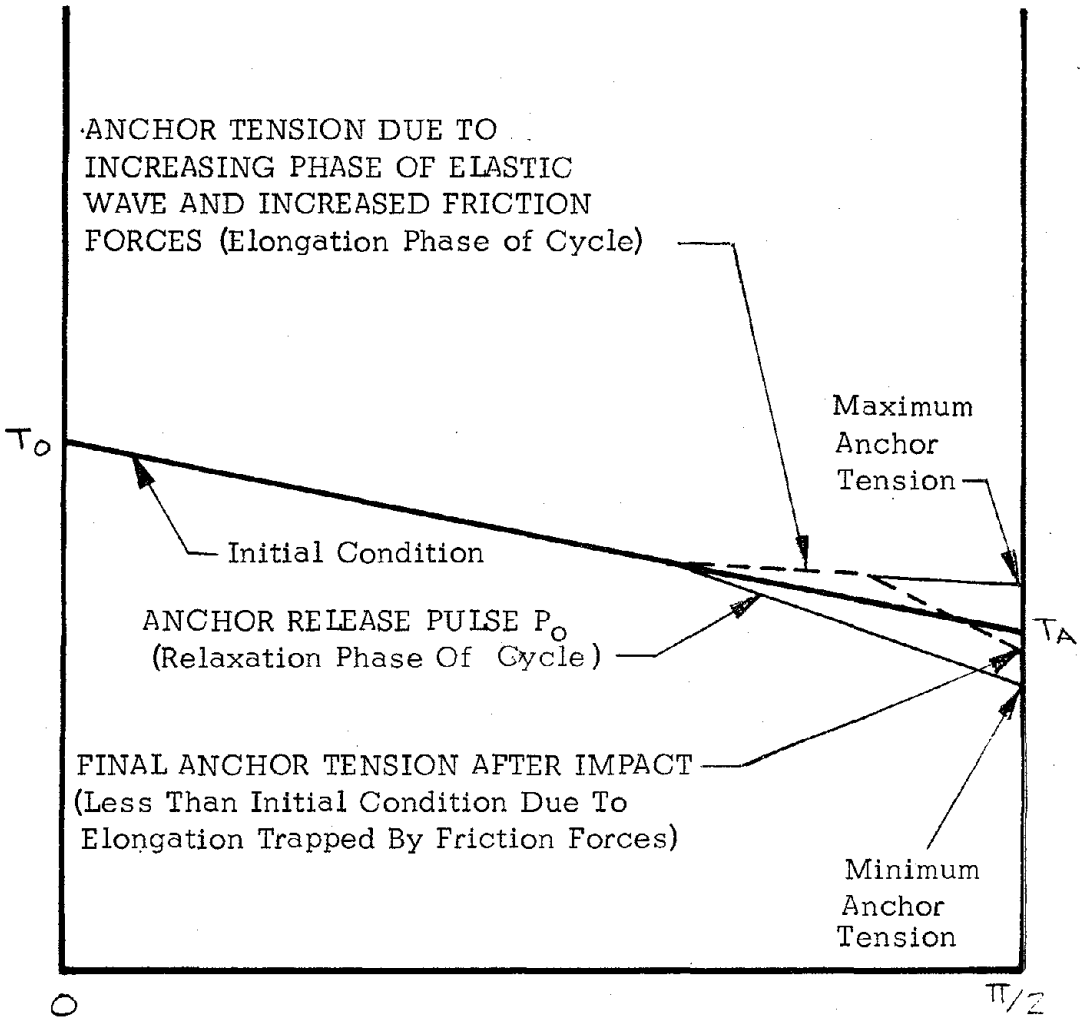

(b) With Reduction in Anchor Tension after Impact.

FIGURE 28. PROBABLE STRESS DISTRIBUTION ALONG TENDON (Continued)

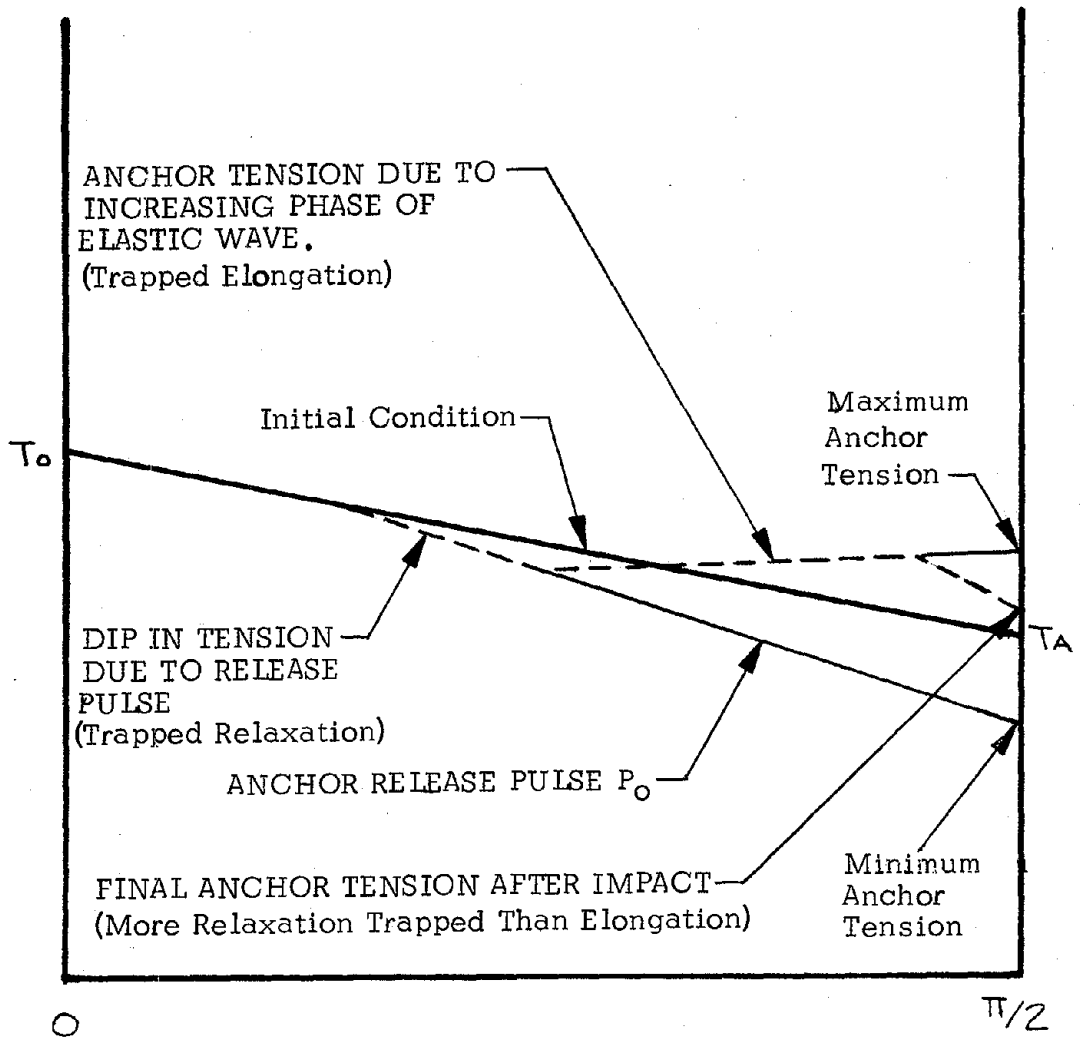

(c) With Increase in Anchor Tension After Impact.

FIGURE 28. PROBABLE STRESS DISTRIBUTION ALONG TENDON (Continued)

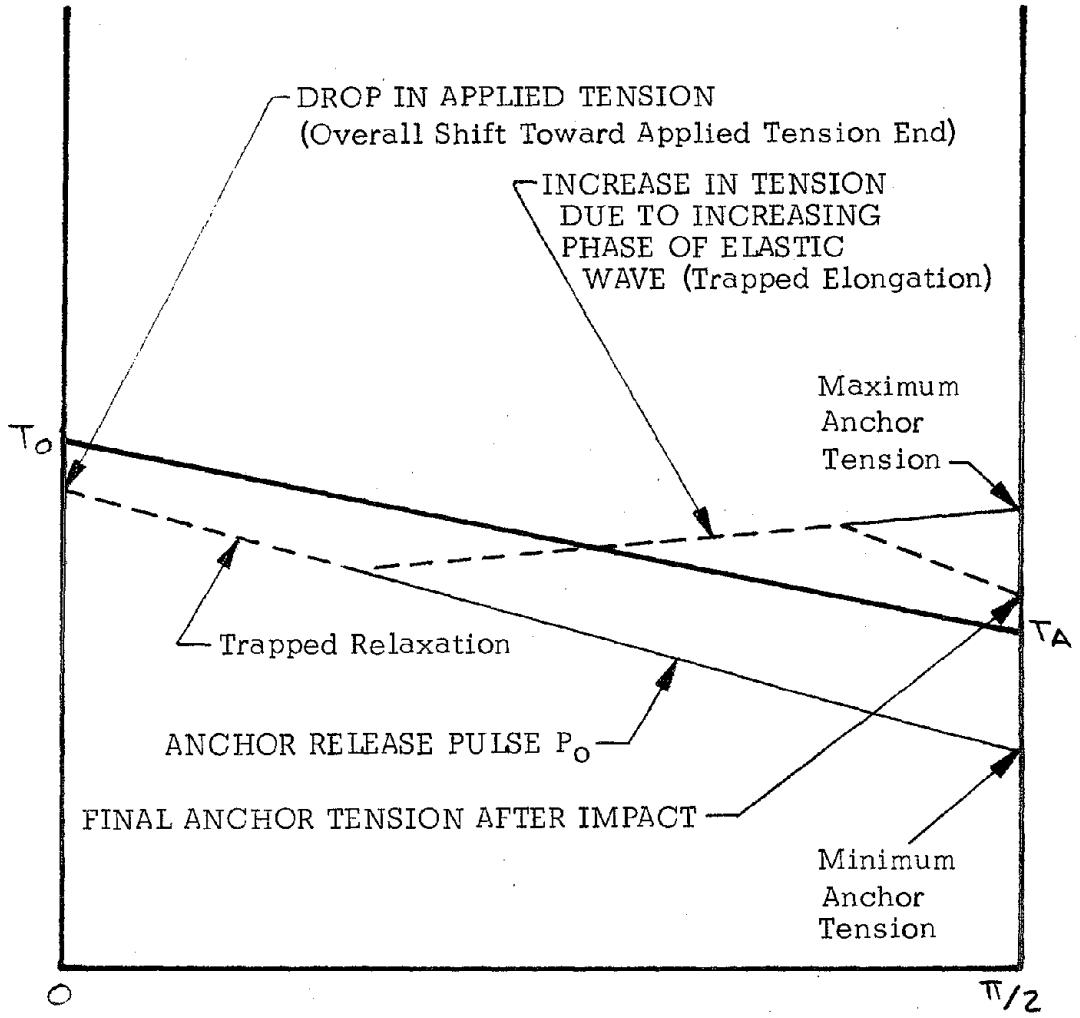

(d) With Reduction in Applied Tension and an Increase in Anchor Tension

FIGURE 23. PROBABLE STRESS DISTRIBUTION ALONG TENDON (Continued)

force at the two ends of the tendon. In the case where the applied tension decreases, and the length of the tendon is greater than a quarter wave length of the generated stress wave, the magnitude of the impact force has been large enough to overcome the static friction force by a given amount, but the magnitude of the applied tension decrease is limited since the anchor end goes into the increasing tension phase of the cycle where friction forces are also increasing. An example of this is shown in Figure 25, where the applied tension decrease is occurring after the anchor impact force has reached its peak magnitude.

The end result of all this is that the friction forces have "captured" a slight displacement in the direction of the applied tension. Since the applied tension is greater than the anchor tension, the drop in applied tension is greater than the change in anchor tension for the same magnitude of displacement. A diagram of the slip-type stress distribution is given in Figure 28 (d) for the moment immediately after impact.

c. Mathematical Model. An approximate mathematical model may be determined if the impulse duration is allowed to increase so that the full effect of the impact is realized. Considering the tendon element of Figure 29, with the initial conditions given by the standard equation for calculating the tension along a post-tensioned tendon:

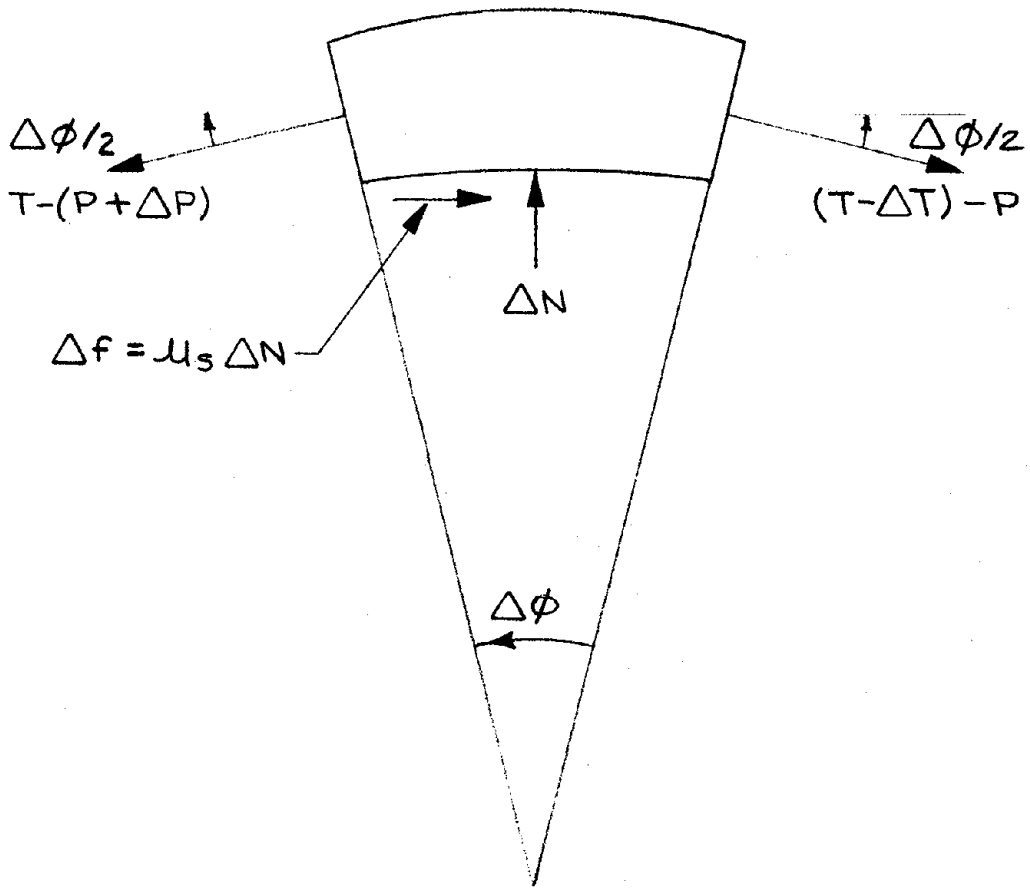

$$[T-(P+\Delta P)]\cos\Delta\phi/2-[(T-\Delta T)-P]\cos\Delta\phi/2-\mu_S\Delta N=0$$

$$[T-(P+\Delta P)]\sin\Delta\phi/2+[(T-\Delta T)-P]\sin\Delta\phi/2-\Delta N=0$$

$$(\Delta T-\Delta P)\cos\Delta\phi/2-\mu_S[2(T-P)-(\Delta T+\Delta P)]\sin\Delta\phi/2=0$$

$$\lim_{\Delta\phi\to 0}\left\{\left(\frac{\Delta T}{\Delta\phi}-\frac{\Delta P}{\Delta\phi}\right)\cos\frac{\Delta\phi}{2}-\mu_S\left[(T-P)-\frac{(\Delta T+\Delta P)}{2}\right]\frac{\sin\Delta\phi/2}{\Delta\phi/2}\right\}$$

$$=\frac{dT}{d\phi}-\frac{dP}{d\phi}-\mu_S(T-P)\quad\text{WHICH GIVES}$$

$$T_L-P_L=(T_A-P_o)\,EXP(\mu_S\phi)\quad(2)$$

FIGURE 29. TENDON ELEMENT WITH INITIAL CONDITIONS T_o AND T_A UNDER THE INFLUENCE OF RELEASE PULSE P_o.

$$T_A = T_o \text{ EXP } (-\mu_k \phi) \qquad (1)$$

Where T_A = anchor tension

T_o = initial tension

μ_k = kinetic friction coefficient

ϕ = total curvature along the tendon

and a long duration square wave type release pulse, an expression for the tension on the tendon may be obtained of the form:

$$T_L - P_S = (T_A - P_o) \text{ EXP } (\mu_s \phi) \qquad (2)$$

Where $T_L = T_o + T_S$ = applied tension + static friction force

P_S = magnitude of decrease in static friction force due to impact

T_A = anchor tension

P_o = impact

μ_s = coefficient of static friction

ϕ = total angular change in radians along cable.

Figure 30 (a) is a diagram of the initial kinetic and static conditions using static and kinetic friction coefficients of 0.4 and 0.2 respectively, and a 30 kip (1.334×10^5 Newton) initial tension. Also in the Figure 30 (a) a 4 kip (1.779×10^4 Newton) release pulse has been superimposed on the initial conditions. The release pulse is cancelled by the static friction force at the point where the friction force becomes greater than the applied tension. Relaxation occurs up to that point, according to the line defined by Equation (2).

When the anchor tension begins to increase, the system is in free damped oscillation so that the resulting anchor tension increase is less than 2 P_o by an amount determined by the damping. If, for illustration purposes, this is controlled to be 1.75 P_o, then the line of the equation:

$$T' = (T_A + .75\ P_o)\ \text{EXP}\ (-\mu_s \phi) \qquad (3)$$

may be added to the diagram of Figure 30 (a). The resulting stress distribution is shown in Figure 30 (b). A dip in tension is seen to occur between the intersection of the curves of equations (2) and (3) with the curve of equation (1).

If the anchor tension is now allowed to decrease back toward T_A, the final anchor tension will settle at a point slightly above T_A, as shown in Figure 30 (c). A hump now occurs because friction retains part of the increase in tension. The anchor tension settles above T_A because more displacement was lost to relaxation in the dip than that gained in the hump. The difference will be reflected by an increase in anchor tension.

If this process were repeated for a system with larger static and kinetic friction coefficients, less displacement would be lost to friction forces for the same magnitude of release pulse. Figure 31 shows this condition. The range of forces allowing an indicated decrease in anchor tension is therefore increased as is exemplified by the data of Tables 7 and 8.

When P_o is large enough to overcome the static friction force, equation (2) takes the kinetic friction coefficient and the applied

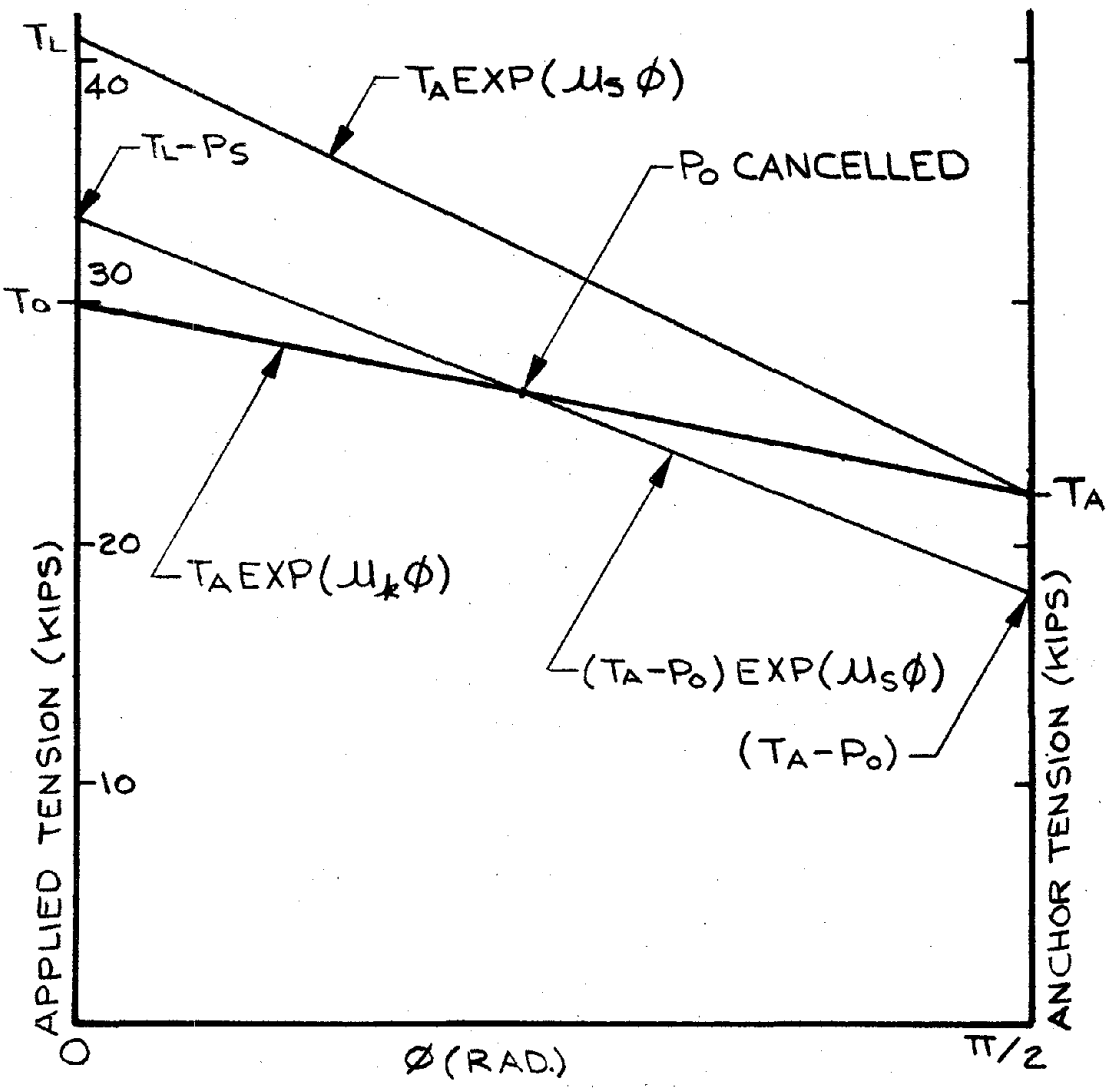

1 kip = 450 kg

(a) With Superimposed Release Pulse P_o.

FIGURE 30. STRESS DISTRIBUTION ALONG TENDON

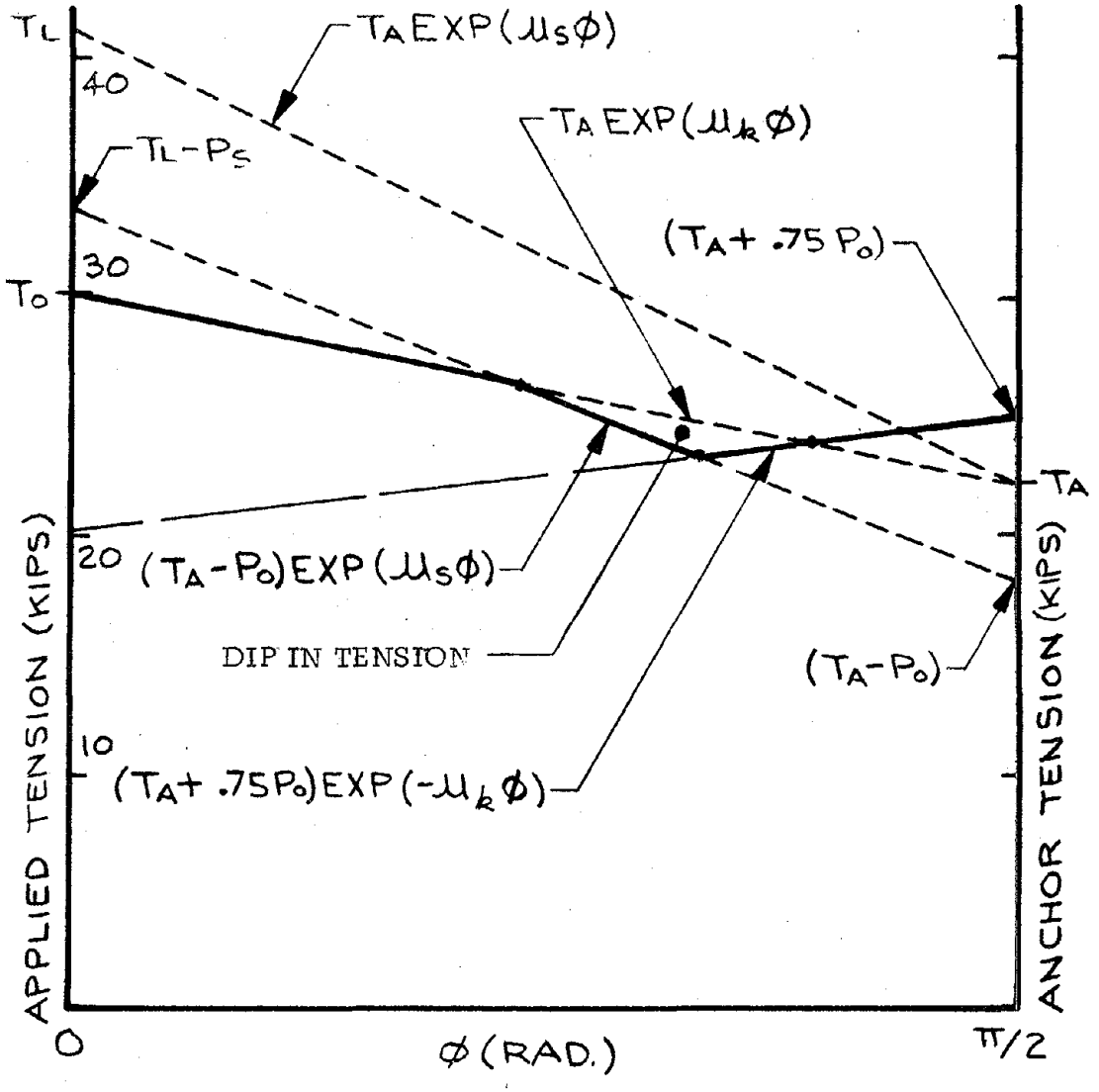

1 kip = 450 kg

(b) After Maximum Elastic Wave.

FIGURE 30. STRESS DISTRIBUTION ALONG TENDON (Continued)

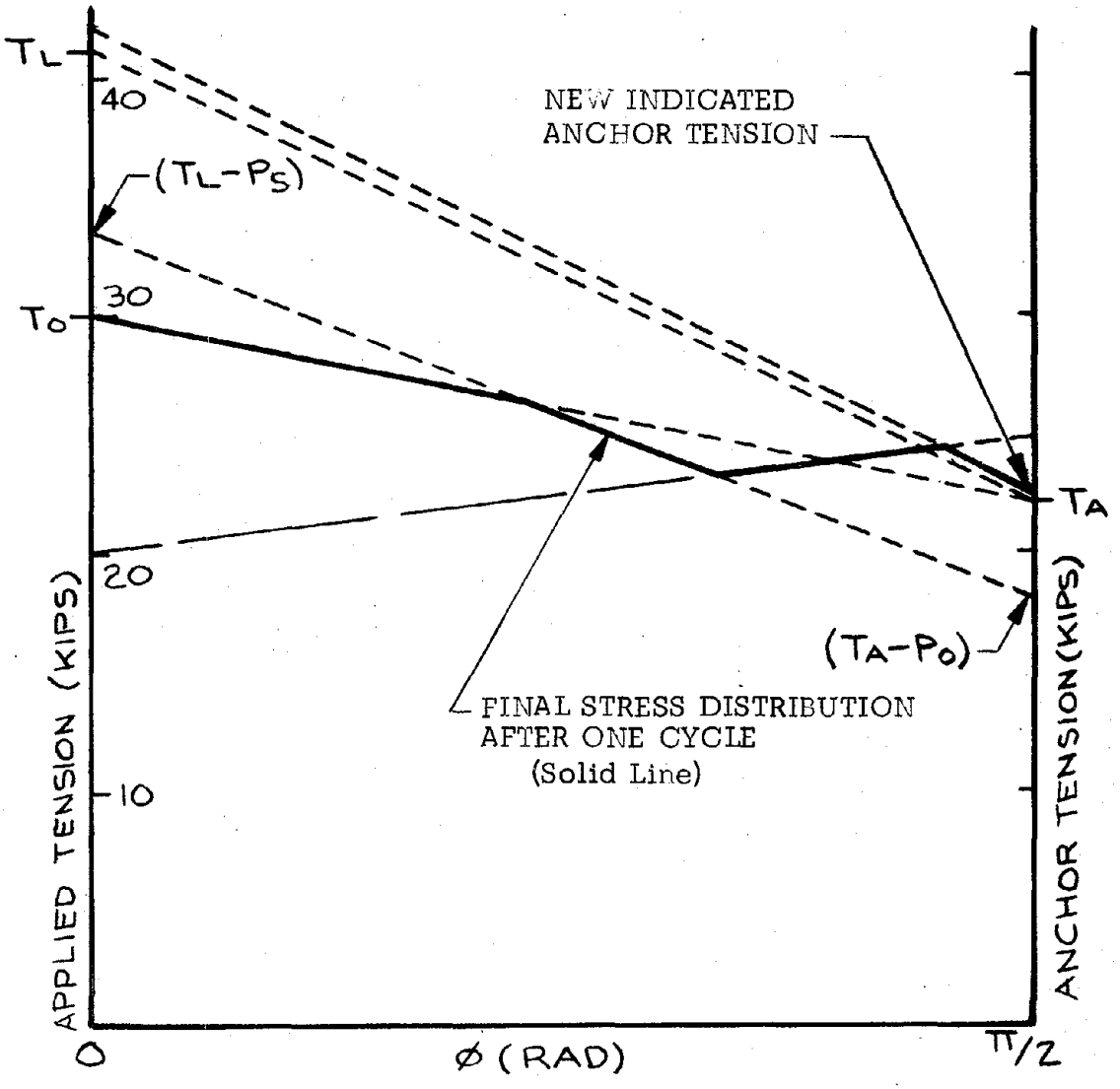

1 kip = 450 kg

(c) After One Cycle of Elastic Wave Generated by Release Pulse P_o.

FIGURE 30. STRESS DISTRIBUTION ALONG TENDON (Continued)

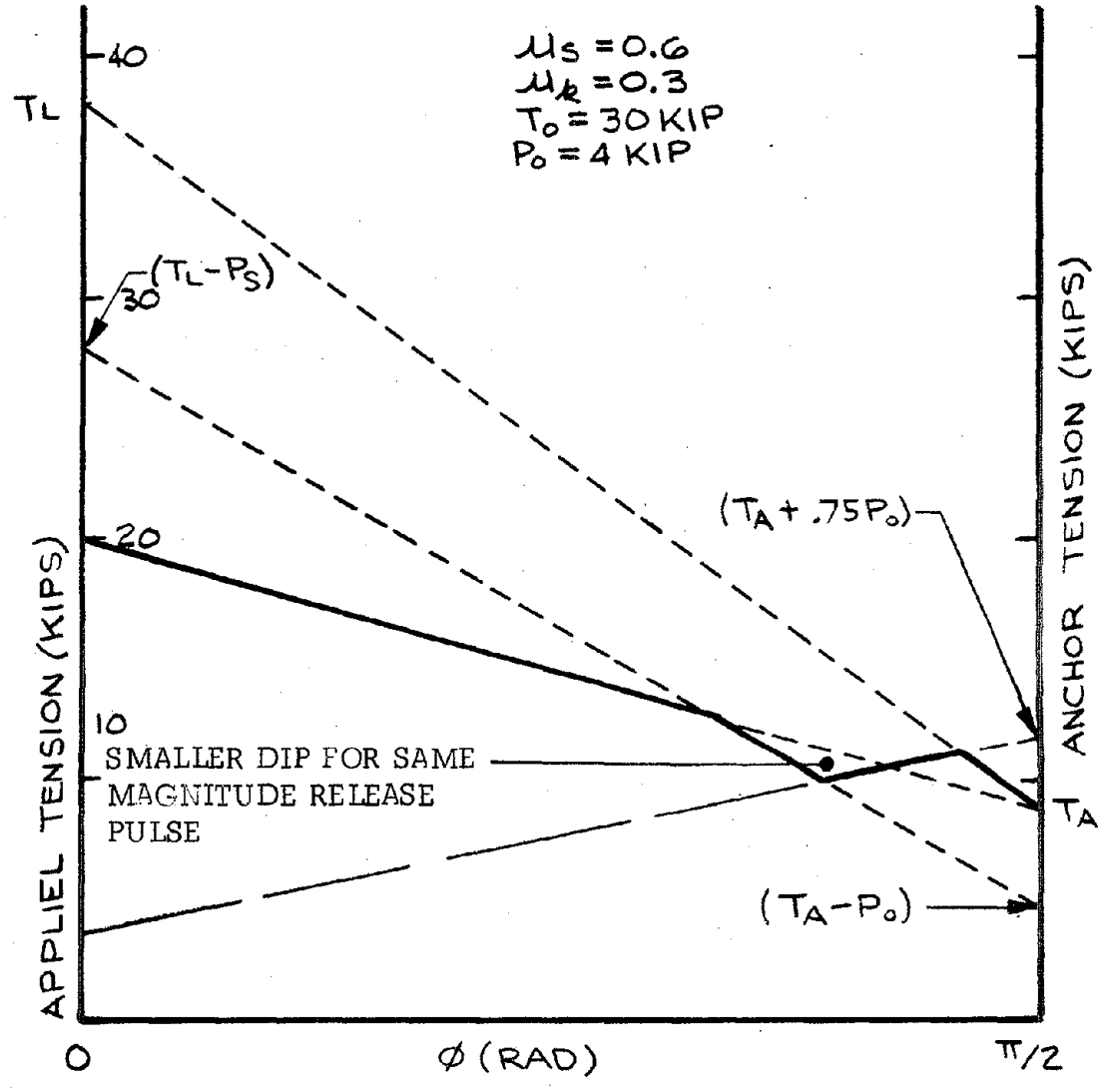

1 kip = 450 kg

FIGURE 31. STRESS DISTRIBUTION FOR HIGHER STATIC AND KINETIC FRICTION CONDITIONS.

tension decreases the allowed amount. The stress distribution after one cycle is shown in Figure 32 before and after retensioning.

Figure 33 shows an approximation of stress distribution after several cycles if P_o were just equal to T_s. After retensioning, however, the stress distribution would come back to the initial conditions.

Recalling the diagrams of Figure 26, the first three figures have now been developed to the actual situations which are confirmed by the data. The desired results of Figure 26 (d), as can be seen from the preceding information, are then not achieved by the impact method and other methods must be sought in order to effectively reduce friction losses for post-tensioned pavements.

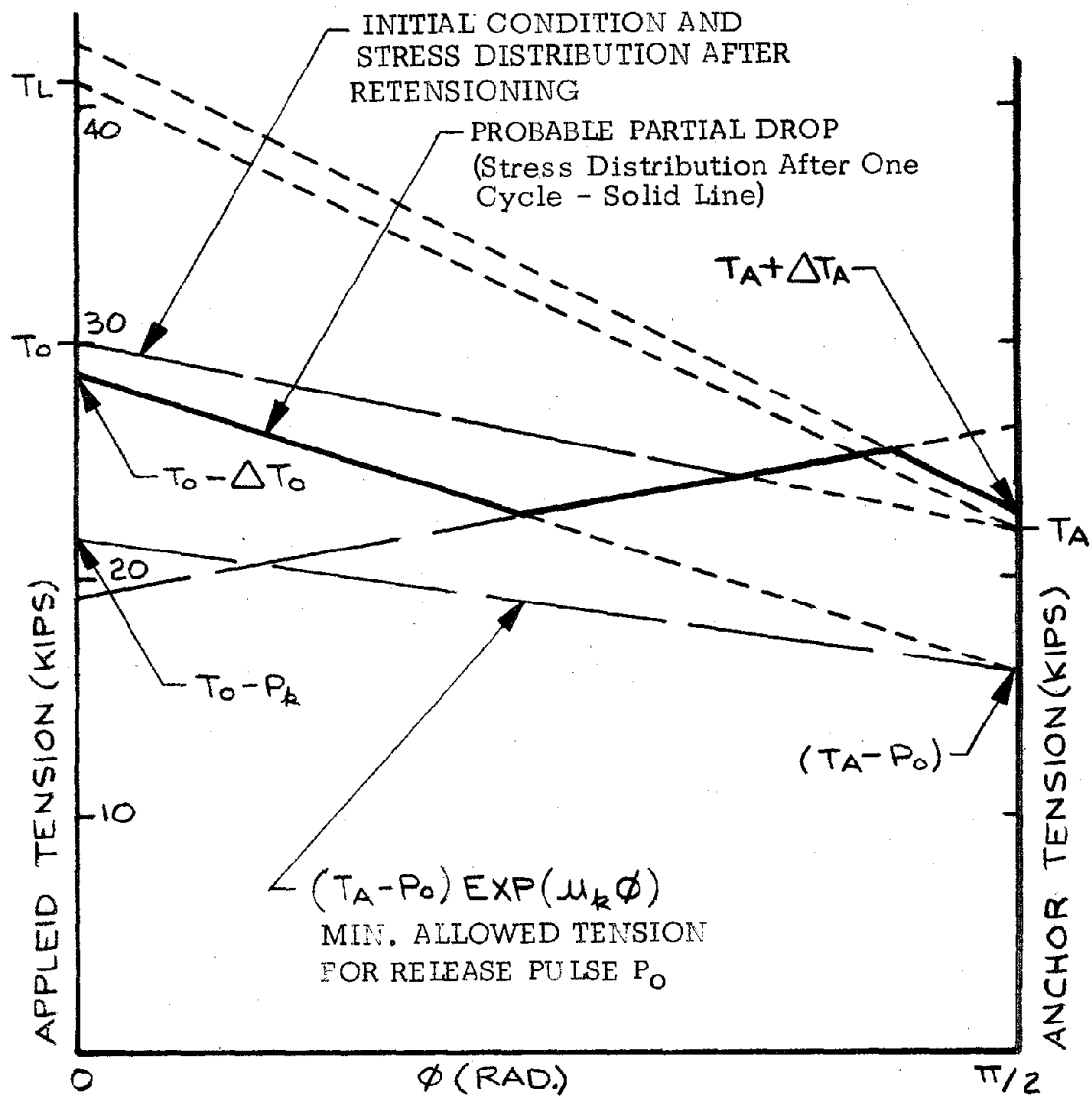

1 kip = 450 kg

FIGURE 32. MAXIMUM TENSION DROP ALLOWED WHEN P_o IS LARGE ENOUGH TO JUST OVERCOME THE STATIC FRICTION BARRIER: PROBABLE PARTIAL DROP WHICH IS SEEN TO OCCUR: STRESS DISTRIBUTION AFTER RETENSIONING.

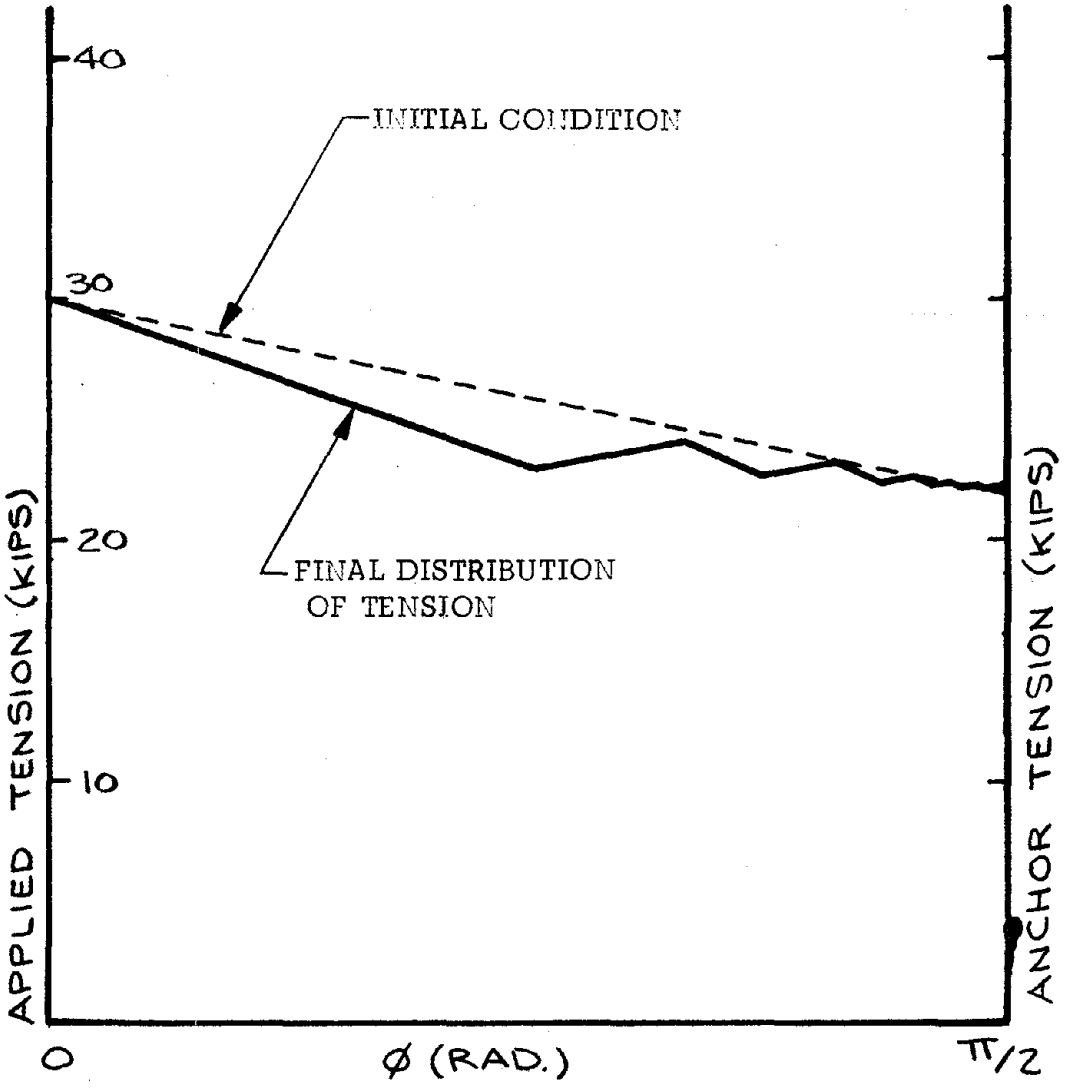

1 kip = 450 kg

FIGURE 33. APPROXIMATE STRESS DISTRIBUTION AFTER SEVERAL CYCLES.

* U.S. GOVERNMENT PRINTING OFFICE: 1978— 621-791/332